

THIS REPORT HAS BEEN DELIMITED
AND CLEARED FOR PUBLIC RELEASE
UNDER DOD DIRECTIVE 5200.20 AND
NO RESTRICTIONS ARE IMPOSED UPON
ITS USE AND DISCLOSURE.

DISTRIBUTION STATEMENT A

APPROVED FOR PUBLIC RELEASE;
DISTRIBUTION UNLIMITED.

Armed Services Technical Information Agency

Because of our limited supply, you are requested to return this copy WHEN IT HAS SERVED YOUR PURPOSE so that it may be made available to other requesters. Your cooperation will be appreciated.

AD

45449

NOTICE: WHEN GOVERNMENT OR OTHER DRAWINGS, SPECIFICATIONS OR OTHER DATA ARE USED FOR ANY PURPOSE OTHER THAN IN CONNECTION WITH A DEFINITELY RELATED GOVERNMENT PROCUREMENT OPERATION, THE U. S. GOVERNMENT THEREBY INCURS NO RESPONSIBILITY, NOR ANY OBLIGATION WHATSOEVER; AND THE FACT THAT THE GOVERNMENT MAY HAVE FORMULATED, FURNISHED, OR IN ANY WAY SUPPLIED THE SAID DRAWINGS, SPECIFICATIONS, OR OTHER DATA IS NOT TO BE REGARDED BY IMPLICATION OR OTHERWISE AS IN ANY MANNER LICENSING THE HOLDER OR ANY OTHER PERSON OR CORPORATION, OR CONVEYING ANY RIGHTS OR PERMISSION TO MANUFACTURE, USE OR SELL ANY PATENTED INVENTION THAT MAY IN ANY WAY BE RELATED THERETO.

Reproduced by

DOCUMENT SERVICE CENTER

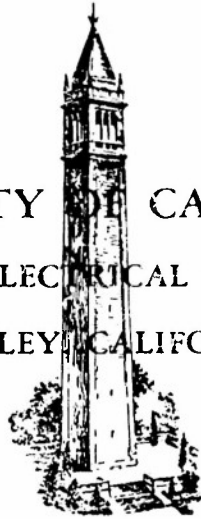
KNOTT BUILDING, DAYTON, 2, OHIO

UNCLASSIFIED

AD No. 405449

ASTIA FILE COPY

UNIVERSITY OF CALIFORNIA
DIVISION OF ELECTRICAL ENGINEERING
BERKELEY, CALIFORNIA



ELECTRONICS RESEARCH LABORATORY

CORNER REFLECTOR STANDARD GAIN ANTENNAS FOR 800 TO 1600 MEGACYCLES

by

James J. Epis

Institute of Engineering Research

Series No. 60, Issue No. 118

July 15, 1954

DIVISION OF ELECTRICAL ENGINEERING
ELECTRONICS RESEARCH LABORATORY

SERIES NO. 60

ISSUE NO. 118

ANTENNA GROUP

Report No. 31 on
Office of Naval Research
Contract N7 onr-29529

CORNER REFLECTOR STANDARD GAIN ANTENNAS
FOR 800 TO 1600 MEGACYCLES

Prepared by:

J. J. Epis
J.J. Epis, Graduate Student

Edited by:

L. E. Reukema
L.E. Reukema, Professor of Electrical Engineering

Approved by:

J. R. Whinnery
J.R. Whinnery, Vice-Chairman, Division of Electrical
Engineering, in charge of the Electronics
Research Laboratory

TABLE OF CONTENTS

I. Introduction	1
II. Considerations on Standard Gain Antennas	3
III. Theoretical Analysis of Corner Reflector Antenna Performance	5
3.1 Determination of the Far-Zone Fields	5
3.2 Equations for the Gain and Radiation Resistance of Corner Reflector Antennas	5
3.3 Solutions of the Radiation Resistance Integral	11
3.3A Radiation Resistance of 90° Corner Reflector Antennas	12
3.3B Radiation Resistance of 60° Corner Reflector Antennas	14
3.3C Radiation Resistance of 45° Corner Reflector Antennas	15
3.3D Radiation Resistance of Other Corner Reflector Antennas	17
3.4 Numerical Evaluation of Radiation Resistance and Antenna Gain	18
3.5 Accuracy of the Calculations	20
IV. The Poynting Vector Method VS. the Circuit Method	23
V. Design of the Corner Reflector Antennas	26
5.1 Factors in the Design	26
5.2 Design Features of the Variable Corner Reflector	28
5.3 The Choice and the Design of the Feed Antenna	29
VI. Transmitting and Receiving Equipment	31
VII. Preliminary Measurements	32
VIII. Two Gain Standards and Their Performances	34
8.1 Selection of the Gain Standards	34
8.2 H-Plane Radiation Patterns of Standard Antenna I and Standard Antenna II	35
8.3 E-Plane Radiation Patterns of Standard Antenna I and Standard Antenna II	36
8.4 Gain Calibrations of Standard Antenna I and Standard Antenna II	37
8.5 Comparison of Calculated and Measured Performance	40
8.6 Future Use of Standard Antennas I and II	42
IX. Summary of Results	43
X. Conclusions	45
Appendix A	46
Appendix B	54
Bibliography	58
Distribution List	59

I INTRODUCTION

Evaluation of the performance of an antenna is generally made by determination of three main quantities; these are the antenna gain, the antenna far-zone field or radiation pattern, and the antenna impedance. In a given evaluation, the relative significance of these quantities will largely depend upon the specific requirements of the transmission system in which the antenna is to be used. The first quantity, namely the gain, is nearly always of considerable importance.

The gain of an antenna is defined as the ratio of the power flux density due to the antenna to the power flux density to an isotropic source radiating equal power. This definition implies that an antenna intrinsically possesses directive properties, or directivity, and implies that the gain is a measure of this directivity. The practical importance of determining the gain of a given antenna lies in the fact that the effectiveness of the antenna in concentrating electromagnetic energy in a favored direction will then be known.

Accurate analytical determinations of antenna gain are usually impractical, if not impossible, excepting those for the relatively few simple-type antennas for which the mathematical relation between antenna aperture distribution, far-zone field, and gain is not overly complicated to determine and solve. Fortunately, several experimental methods of determining the gain have been devised, the most important methods being the two antenna method, the mirror method, and the comparison method.^{1, 2a, 3}

Two identical antennas are used in the first of the above experimental methods; the ratio of the power transmitted by either antenna to that received by its counterpart is measured. In the mirror method, the ratio of the power transmitted by the antenna under test to the power received by that antenna as a consequence of direct reflection from a planar metallic sheet or electromagnetic mirror is measured. In the comparison method, as its name may imply, a comparison is made of power radiated or received by the antenna under test with that radiated or received by a second antenna of known gain. The gain of the test antenna is easily arrived at from such a comparison; in fact, the comparison method is almost always the simplest and the most convenient of the three

methods considered. The auxiliary antennas employed in comparison measurements are appropriately called standard gain antennas, or simply, standard antennas. Needless to say, these antennas are very useful and valuable.

The accuracy of a comparison measurement obviously depends to a large extent on the accuracy of the known value of gain of the standard antenna. Therefore, it is of paramount importance that a developmental standard antenna be calibrated as accurately as possible. This calibration is necessarily accomplished employing the relatively cumbersome two antenna or mirror methods.

The research described in the thesis to follow is concerned with the development of corner reflector antennas as standard gain antennas. In the first section, considerations related to standard antennas are discussed and arguments justifying the selection of corner reflector antennas for investigation are given. In succeeding sections, a comprehensive theoretical analysis on the performance of corner reflector antennas is presented and calculated performance is compared with measured performance. Included are the calculated and measured performances of two corner reflector antennas proposed as gain standards.

The two-fold objective of this research is to investigate analytically and experimentally the performance of corner reflector antennas and to discover and calibrate corner reflector antenna prototypes suitable for usage as standard gain antennas particularly for 800 to 1600 megacycles.

II CONSIDERATIONS ON STANDARD GAIN ANTENNAS

Very often, the main factor which determines the value of a standard gain antenna is the width of the frequency band for which its gain is accurately calibrated. This statement may be appreciated since the utility of a standard antenna calibrated over a narrow frequency band will be limited unless several specialized antennas intended for a single frequency, or for a narrow band of frequencies, are to be investigated extensively.

It follows that an antenna possessing a favorable gain vs frequency characteristic is to be desired for development as a gain standard. The gain vs frequency characteristic described below is considered favorable:

- (1) A constancy in gain for an appreciable frequency band, or for the calibration band of the (proposed) gain standard.
- (2) An average value of gain the same order of magnitude as the (estimated) average of the gains of a wide selection of antennas already used or likely to be used at frequencies in the calibration band.

Explanation of the importance of (1) and (2) is given in the succeeding paragraph.

An important aspect of the comparison method is that quite often it is difficult to make accurate gain comparisons if the gains of the standard antenna and the test antenna are separated by more than about 10 db.* Now the standard antenna will likely be used at all frequency regions in its calibration band. Therefore, the chance of encountering cases wherein the above mentioned (or the actual) limiting decibel separation in gain is reached will obviously be smaller, the closer the performance of the standard antenna resembles that of (1) and (2).

Another factor deserving consideration is the impedance of the antenna. This factor is important because the antenna must be matched to its transmission line during calibration and also during future use as a gain standard. Low-loss, broad-band impedance matching transformers capable of matching appreciable voltage standing wave ratios are fairly common; therefore, the broad-band impedance is not as important to this discussion as broad-band gain.

*It is noteworthy to mention that this limitation is placed solely by the limitations on sensitivity and/or linearity and/or noise figure of power measuring equipment in common use.

It can be argued that for development as a gain standard it is advantageous to select an antenna whose gain is calculable to a good first-approximation. Gain as a function of frequency will depend on one or more antenna parameters: antenna lengths, flare angles, focal lengths, aperture geometries, etc., are examples. Attainment of the most favorable broad-band gain characteristic is of course coincident with the discovery of the optimum combination of settings of the antenna parameters. This discovery is likely to require considerably less combined effort if the gain is accurately calculable, since experimental gain calibrations need be made only for a small range of parameter settings about those calculated to be optimum.

One simple-type antenna for which accurate calculation of gain is possible is the dihedral corner reflector. This is one reason corner reflector antennas were selected for the research to be described. But more significant, according to Kraus¹, dipole-fed corner reflector antennas have acceptable broad-band gain and impedance characteristics for a number of combinations of settings of corner angle and corner to dipole spacing. In addition, important practical advantages favoring corner reflector antennas are their simplicity of construction and consequently, their relatively low cost.

III THEORETICAL ANALYSIS OF CORNER REFLECTOR

ANTENNA PERFORMANCE

3.1 Determination of the Far-Zone Fields

Previous analyses on the far-zone fields of corner reflector antennas have been repetitious in that a separate calculation is made for each corner angle considered. These calculations are rather lengthy if the corner angle is smaller than 90° .^{*} The purpose of the analysis which follows is to derive the general solution for the far-zone field of a corner reflector antenna, that is, the solution valid for all corner angles.

It is assumed, as in previous analyses, that the antenna structure consists of two infinite intersecting sheets of infinitely conductive metal. Of course, this assumption is equivalent to neglecting ohmic losses and edge effects or diffraction about the ends of the reflector of a practical (finite) corner reflector. In addition, the corner angle (α) is restricted to the infinite set of values $\alpha = \frac{2\pi}{m}$, m being any even integer. This restriction — which also is present in previous analyses — is made so that the well known theory of images⁶ may be employed.

The figures on the following page illustrate the co-ordinate systems that are used and the locations of the corner reflector, feed antenna, and images of the feed antenna. The unit vectors, image-numbering system, and various constants used in the analysis are also illustrated.

The total field at a distant point $P(R, \theta, \phi)$, or $P(x, y, z)$ is the vector resultant of the fields due to the feed antenna and its various images. Of course, phase differences in the excitation of the images and phase differences arising from the space variance in the distances from the images to the field point must be taken into account in this vector summation. In this regard, Fig. 2 illustrates that the excitation of the feed antenna — to be denoted as "image" No. 1 — and images 5, 9, 13, 17, etc., is positive while that of images 3, 7, 11, 15, etc., is negative. The phase of the excitation of the even-numbered images is considered to be arbitrary (positive or negative) at the beginning of the analysis; the correct phase will be chosen at a convenient interval.

From the above discussion, it follows that the fields due to pairs of diametrically opposite images are:

^{*}For an example, see reference No. 5 of the Bibliography.

$$\bar{E}_1 + \bar{E}_2 = \bar{E}_0 (e^{jks \bar{i}_0 \cdot \bar{i}_r} + e^{-jks \bar{i}_0 \cdot \bar{i}_r})$$

$$\bar{E}_3 + \bar{E}_4 = -\bar{E}_0 (e^{jks \bar{i}_1 \cdot \bar{i}_r} + e^{-jks \bar{i}_1 \cdot \bar{i}_r})$$

$$\bar{E}_5 + \bar{E}_6 = \bar{E}_0 (e^{jks \bar{i}_2 \cdot \bar{i}_r} + e^{-jks \bar{i}_2 \cdot \bar{i}_r})$$

$$\bar{E}_7 + \bar{E}_8 = -\bar{E}_0 (e^{jks \bar{i}_3 \cdot \bar{i}_r} + e^{-jks \bar{i}_3 \cdot \bar{i}_r})$$

etc.,

$$\bar{E}_{m-1} + \bar{E}_m = (-1)^{\frac{m}{2}-1} \bar{E}_0 (e^{jks \bar{i}_{\frac{m}{2}-1} \cdot \bar{i}_r} + e^{-jks \bar{i}_{\frac{m}{2}-1} \cdot \bar{i}_r})$$

where:

(1). \bar{E}_0 = Field at $P(R, \theta, \phi)$, of the feed antenna radiating in free space when excited with the current distribution it possesses in the presence of the corner reflector;

(2). $\bar{E}_1 + \bar{E}_2$ = Fields at $P(R, \theta, \phi)$ due to images 1 and 2

$\bar{E}_3 + \bar{E}_4$ = Fields at $P(R, \theta, \phi)$ due to images 3 and 4, etc.,

$\bar{E}_{m-1} + \bar{E}_m$ = Fields at $P(R, \theta, \phi)$ due to image $m-1$ and image m ;

(3). \bar{i}_r = Unit vector in the direction of the field point

\bar{i}_0 = Unit vector in the direction of image 1

$-\bar{i}_0$ = Unit vector in the direction of image 2

\bar{i}_1 = Unit vector in the direction of image 3

$-\bar{i}_1$ = Unit vector in the direction of image 4, etc.,

$\bar{i}_{\frac{m}{2}-1}$ = Unit vector in the direction of image $m-1$

$-\bar{i}_{\frac{m}{2}-1}$ = Unit vector in the direction of image m ;

(4). $K = 2\pi/\lambda$, λ = the wavelength.

Summing the fields of the m images gives the resultant field \bar{E} , as follows:

$$\bar{E} = (\bar{E}_1 + \bar{E}_2) + (\bar{E}_3 + \bar{E}_4) + \dots + (\bar{E}_{m-1} + \bar{E}_m), \text{ or}$$

$$\bar{E} = \sum_{n=0}^{\frac{m}{2}-1} (-1)^n \bar{E}_0 (e^{jks \bar{i}_n \cdot \bar{i}_r} + e^{-jks \bar{i}_n \cdot \bar{i}_r}) \quad (1)$$

Now, it is seen from Fig. 2, that $\bar{i}_0 = \bar{i}_x$, $\bar{i}_1 = \cos \frac{2\pi}{m} \bar{i}_x$

$+ \sin \frac{2\pi}{m} \bar{i}_y$, $\bar{i}_2 = \cos \frac{4\pi}{m} \bar{i}_x + \sin \frac{4\pi}{m} \bar{i}_y$, etc., and

$$\bar{i}_n = \cos \frac{2\pi n}{m} \bar{i}_x + \sin \frac{2\pi n}{m} \bar{i}_y$$

Substituting these unit vectors in equation (1) yields

$$\bar{E} = \sum_{n=0}^{\frac{m}{2}-1} (-1)^n \bar{E}_0 \left\{ \exp. \left[jks \left(\cos \frac{2\pi n}{m} \bar{i}_x + \sin \frac{2\pi n}{m} \bar{i}_y \right) \cdot \bar{i}_r \right] \right. \\ \left. + \exp. \left[-jks \left(\cos \frac{2\pi n}{m} \bar{i}_x + \sin \frac{2\pi n}{m} \bar{i}_y \right) \cdot \bar{i}_r \right] \right\}$$

But $\bar{i}_x \cdot \bar{i}_r = \sin \theta \cos \phi$ and $\bar{i}_y \cdot \bar{i}_r = \sin \theta \sin \phi$,

so that

$$\bar{E} = \sum_{n=0}^{\frac{m}{2}-1} (-1)^n \bar{E}_0 \left\{ \exp. \left[jks \sin \theta \left(\cos \frac{2\pi n}{m} \cos \phi + \sin \frac{2\pi n}{m} \sin \phi \right) \right] \right. \\ \left. + \exp. \left[-jks \sin \theta \left(\cos \frac{2\pi n}{m} \cos \phi + \sin \frac{2\pi n}{m} \sin \phi \right) \right] \right\}$$

Or

$$\bar{E} = \sum_{n=0}^{\frac{m}{2}-1} (-1)^n \bar{E}_0 \left\{ \exp. \left[jks \sin \theta \cos \left(\frac{2\pi n}{m} - \phi \right) \right] \right. \\ \left. + \exp. \left[-jks \sin \theta \cos \left(\frac{2\pi n}{m} - \phi \right) \right] \right\}$$

Now, Figs. 3 and 4 on page 7A illustrate the following: corner reflectors having corner angles such that $m = 4, 8, 12, 16$, etc., have diametrically opposite images excited in phase, and consequently, the positive sign must be chosen for the second term in the above summation; whereas, corner reflectors having corner angles such that $m = 2, 6, 10, 14$, etc., have diametrically opposite images excited 180° out of phase so that the negative sign must be chosen. The final results, therefore, are given by equations (2) and (3) below:

$$E = 2E_0 \sum_{n=0}^{\frac{m}{2}-1} (-1)^n \cos \left\{ \left[ks \sin \theta \right] \left[\cos \left(\frac{2\pi n}{m} - \phi \right) \right] \right\} \quad (2)$$

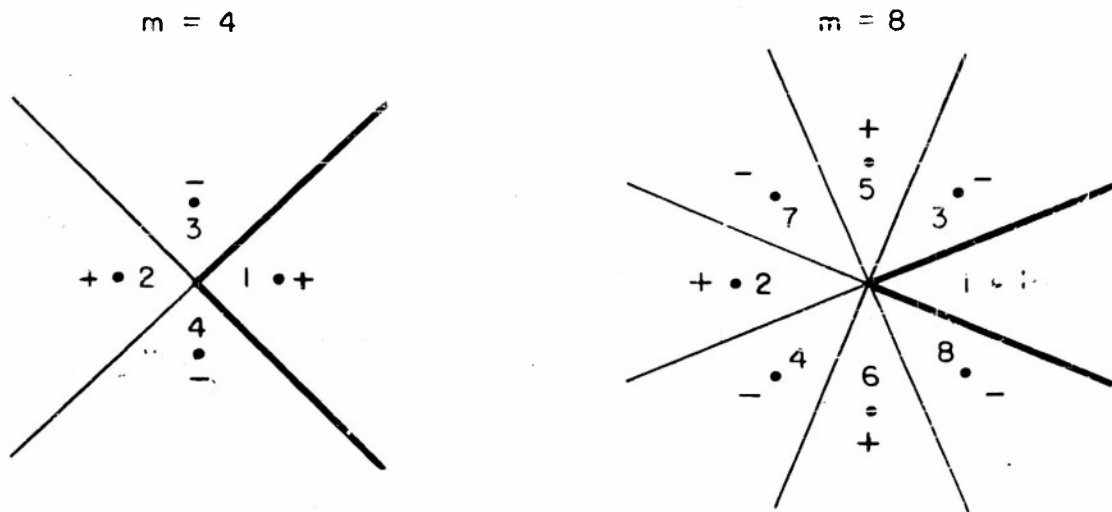


FIG. 3 DIAMETRICALLY OPPOSITE IMAGES EXCITED IN PHASE
($m=4, 8, 12, 16$ etc.)

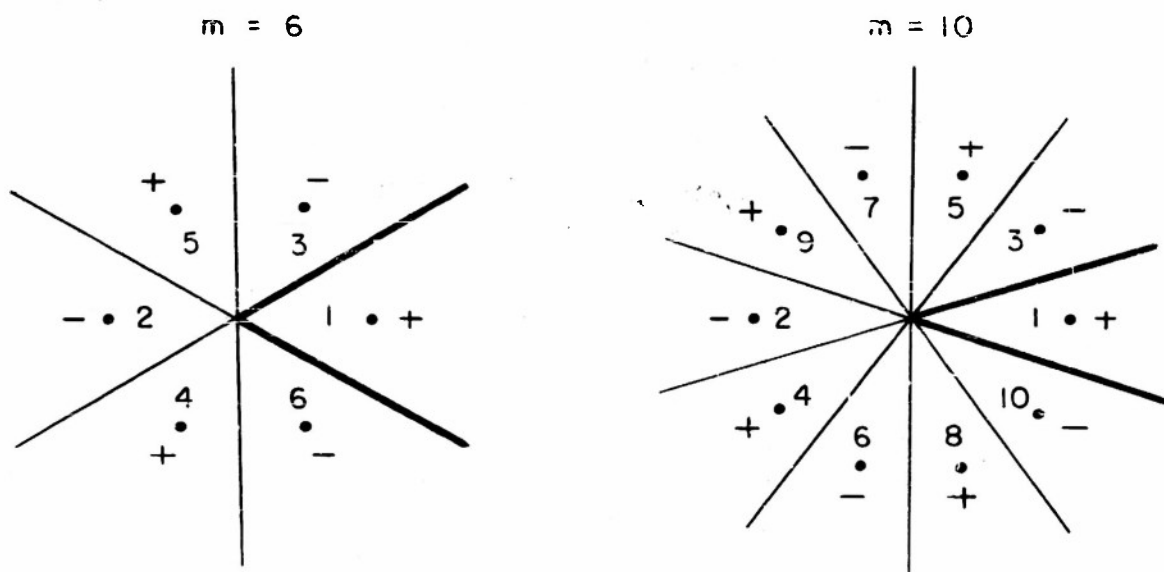


FIG. 4 DIAMETRICALLY OPPOSITE IMAGES EXCITED 180° OUT OF PHASE
($m=2, 6, 10$, etc.)

where: $m = 4, 8, 12, 16 \dots$ for corner angles of $90^\circ, 45^\circ, 30^\circ, 22\frac{1}{2}^\circ \dots$

$$\bar{E} = 2j\bar{E}_0 \sum_{n=0}^{m/2-1} (-1)^n \sin \left\{ [ks \sin \theta] \left[\cos \frac{2\pi n}{m} - \phi \right] \right\} \quad (3)$$

where: $m = 2, 6, 10, 14 \dots$ for corner angles of $180^\circ, 60^\circ, 36^\circ, 25.714^\circ \dots$

It is apparent that equations (2) and (3) give the far-zone fields of all corner reflector antennas having corner angles for which image theory is applicable.

3.2 Equations for the Gain and Radiation Resistance of Corner Reflector Antennas

The gain of any antenna may be defined by the equation

$$G = \frac{4\pi R^2 S(\theta_0, \phi_0)}{P_T} = \frac{4\pi S(\theta_0, \phi_0)}{\int_A S(\theta, \phi) \sin \theta \, d\phi \, d\theta} \quad (4)$$

where: G = The antenna gain in the direction of θ_0, ϕ_0

A = Surface of a distant sphere of radius R

$S(\theta, \phi)$ = Magnitude of the component normal to A
of the time-averaged Poynting vector

P_T = Total power radiated = $R^2 \int_A S(\theta, \phi) \sin \theta \, d\phi \, d\theta$

For the corner reflector antennas, it is convenient to introduce the radiation resistance in the calculation of antenna gain. Radiation resistance will be defined by equation (5), below:

$$R_r = \frac{2 P_T}{I_0^2} = \frac{2 R^2}{I_0^2} \int_A S(\theta, \phi) \sin \theta \, d\phi \, d\theta \quad (5)$$

In this equation, I_0 is the amplitude of the current at a convenient location on the feed antenna, or in the transmission line, and R_r is the radiation resistance referred to the particular I_0 selected.

Because a field — and therefore, the Poynting vector $S(\theta, \phi)$ — is non-existent in all of space behind the metal sheets of the (infinite) corner reflector, the phi limits of integration of the preceding integral may be reduced to the values $-\alpha/2, \alpha/2$, so that

$$R_r = \frac{2R^2}{I_0^2} \int_0^\pi \int_{-\alpha/2}^{\alpha/2} S(\theta, \phi) \sin \theta \, d\phi \, d\theta \quad (6)$$

Now, $S(\theta, \phi) = \frac{\bar{\mathbf{E}} \cdot \bar{\mathbf{H}}}{2} = \frac{\bar{\mathbf{E}} \cdot \bar{\mathbf{H}}}{2\eta} = \frac{|\bar{\mathbf{E}}|^2}{2\eta}$ where $\bar{\mathbf{H}}$ is the magnetic field and η is the intrinsic impedance. In free space $\eta = 120\pi$, and therefore,

$S(\theta, \phi) = \frac{|\bar{\mathbf{E}}|^2}{240\pi} = \frac{|\bar{\mathbf{E}}_0|^2}{60\pi} f^2(s, \theta, \phi)$ where $f(s, \theta, \phi)$ denotes the summation in either equation (1) or equation (2), as the case requires. By substituting

this value of $S(\theta, \phi)$ into equation (6) there is obtained

$$R_r = \frac{R^2}{30\pi I_0^2} \int_0^\pi \int_{-a/2}^{a/2} [|\bar{E}_0|^2 \sin \theta] f^2(s, \theta, \phi) d\phi d\theta \quad (7)$$

The above integral will be transformed through use of the existing symmetry relations. Consider the case of a 90° corner reflector. Lobe No. 1 in Fig. 5 on the following page is radiated by the 90° corner reflector antenna. On the other hand, all four of the lobes shown in the figure are radiated by an array of four sources located in free space and excited and spaced in the same manner as the feed antenna and its images. Therefore, the power radiated by the 90° corner reflector antenna is one-fourth of that radiated by the array. Moreover, because of the symmetry, the power radiated in the upper space domain, $0 \leq \theta \leq \pi/2$, is equal to that radiated in the lower space domain, $\pi/2 \leq \theta \leq \pi$; and identical amounts of power are radiated in each of the domains $0 \leq \phi \leq \pi/4$ and $0 > \phi \geq -\pi/4$. It follows that the theta limits of integration of the preceding integral may be changed to 0, $\pi/2$, and the phi limits to 0, 2π if the integral is multiplied by $(2)(1/4) = 1/2$.

For convenience, the symmetry relations were presented for $\alpha = 90^\circ$. Obviously similar relations exist for all α , and as a consequence, the limits of integration may be changed to the values given above provided that a multiplication factor of $2/m$ is used. The radiation resistance is therefore given by the equation

$$R_r = \frac{R^2}{15\pi I_0^2} \int_0^{\pi/2} \int_0^{2\pi} \{ |\bar{E}_0|^2 \sin \theta \} f^2(s, \theta, \phi) d\phi d\theta \quad (8)$$

The integral in equation (8), hereafter, will be referred to as "the radiation resistance integral".

From equations (4) and (5) it follows that the antenna gain is determined from the radiation resistance by using the equation

$$G(\theta_0, \phi_0) = \frac{8\pi R^2 S(\theta_0, \phi_0)}{I_0^2 R_r} = \left[\frac{2}{15R_r} \right] \left[\frac{R^2 |\bar{E}_0|^2 f^2(s, \theta_0, \phi_0)}{I_0^2} \right] \quad (9)$$

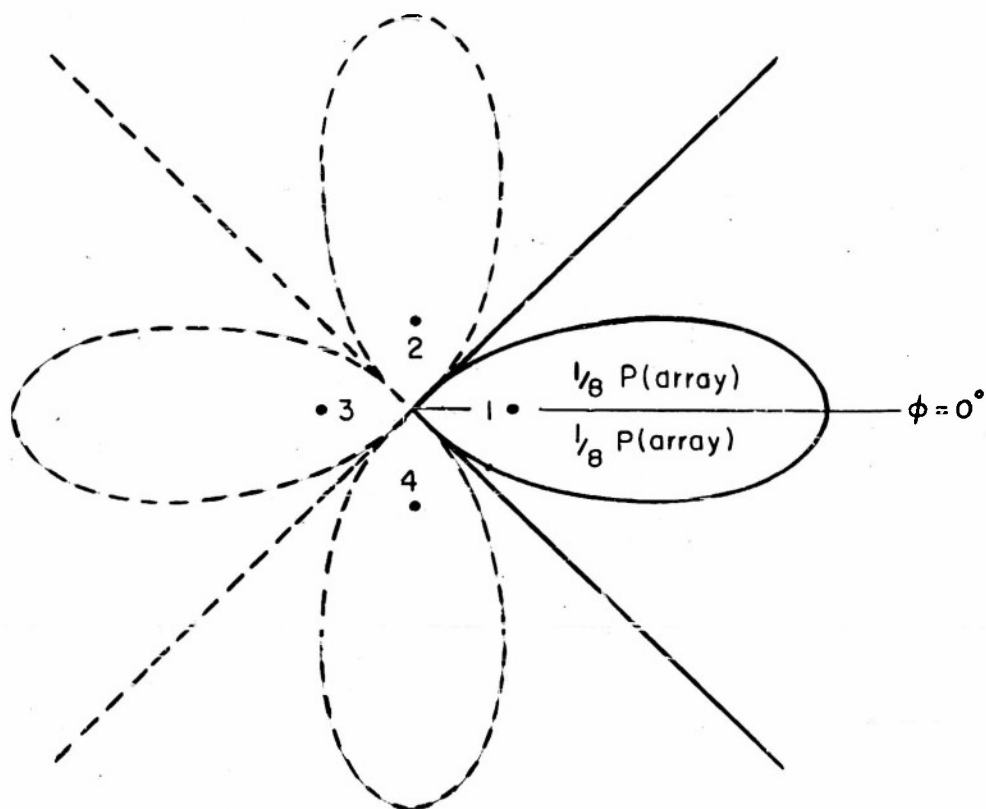


FIG. 5 SYMMETRY BETWEEN RADIATION PATTERNS OF 90°-CORNER REFLECTOR ANTENNA AND FOUR-ELEMENT ARRAY

3.3 Solutions of the Radiation Resistance Integral

As will be demonstrated shortly, integration with respect to ϕ of the radiation resistance integral requires the solutions of the integrals

$$I_1 = \int_0^{\pi/2} \frac{2 [\cos(b \cos \theta) - \cos b]^2 d\theta}{\sin \theta}, \quad I_2 = \int_0^{2\pi} \cos[z \cos(\phi - c)] d\phi,$$

$$I_3 = \int_0^{2\pi} \left\{ \sin[\rho \cos(\phi - b)] \right\} \left\{ \sin[\rho \cos(\phi - a)] \right\} d\phi, \quad \text{and}$$

$$I_4 = \int_0^{2\pi} \left\{ \cos[\rho \cos(\phi - b)] \right\} \left\{ \cos[\rho \cos(\phi - a)] \right\} d\phi, \quad \text{where}$$

$a, b, c, z,$ and ρ are constants. Rigorous derivations of the solutions of these integrals are found in Appendix A. The solutions are included below in order to facilitate their reference in the analyses which follow.

$$I_1 = \left\{ \left[\gamma + \ln 2b + \text{Ci}(2b) \right] + \frac{1}{2} \sin 2b \left[\text{Si}(4b) - \text{Si}(2b) \right] \right. \\ \left. + \frac{1}{2} \cos 2b \left[\gamma + \ln b + \text{ci}(4b) - 2 \text{ci}(2b) \right] \right\}$$

$$I_2 = 2\pi J_0(z)$$

$$I_3 = \pi \left\{ J_0 \left[2\rho \sin \left(\frac{a-b}{2} \right) \right] - J_0 \left[2\rho \cos \left(\frac{a-b}{2} \right) \right] \right\}$$

$$I_4 = \pi \left\{ J_0 \left[2\rho \sin \left(\frac{a-b}{2} \right) \right] + J_0 \left[2\rho \cos \left(\frac{a-b}{2} \right) \right] \right\}$$

In these solutions γ = Euler's Constant, Ci = the cosine integral, Si = the sine integral, J_0 = the zero order Bessel function of the first kind.

The radiation resistance of corner reflector antennas for several values of corner angle is to be derived. The first case considered is $\alpha = 90^\circ$ or $m = 4$.

3.3A - Radiation Resistance of 90° Corner Reflector Antennas

Substituting in the radiation resistance integral the summation in equation 2, page 7, gives

$$R_r = \frac{R^2}{60\pi I_0^2} \int_0^{\pi/2} \int_0^{2\pi} \left\{ |\bar{E}_0|^2 \sin \theta \right\} \left\{ \sum_{n=0}^{\infty} (-1)^n \cos[ks \sin \theta \cos(\frac{n\pi}{2} - \phi)] \right\}^2 d\phi d\theta$$

$$R_r = \frac{R^2}{60\pi I_0^2} \int_0^{\pi/2} \int_0^{2\pi} \left\{ |\bar{E}_0|^2 \sin \theta \right\} \left\{ \cos^2 [\theta \cos \phi] \right. \\ \left. - 2 \cos [\theta \cos \phi] \cos [\theta \cos(\frac{\pi}{2} - \phi)] + \cos^2 [\theta \cos(\frac{\pi}{2} - \phi)] \right\} d\phi d\theta$$

where: $\theta \equiv ks \sin \theta$

Using $\cos^2 B = \frac{1}{2} + \frac{1}{2} \cos 2B$, the last integral becomes

$$R_r = \frac{R^2}{60\pi I_0^2} \int_0^{\pi/2} \int_0^{2\pi} \left\{ |\bar{E}_0|^2 \sin \theta \right\} \left\{ 1 + \left(\frac{1}{2}\right) \cos[2\theta \cos \phi] + \frac{1}{2} \cos[2\theta \cos(\frac{\pi}{2} - \phi)] \right. \\ \left. - \left(2 \cos[\theta \cos \phi] \cos[\theta \cos(\frac{\pi}{2} - \phi)] \right) \right\} d\phi d\theta$$

Now, corner reflector antennas having feed antennas excited uniformly with azimuth are of chief interest in this study; the free-space fields (\bar{E}_0) of these feed antennas are not functions of phi. Consequently, for these cases, the integral above can be integrated with respect to phi by using the solutions of integrals I_2 and I_4 given on page 11. There is obtained

$$R_r = \frac{R^2}{60\pi I_0^2} \left\{ 2\pi \int_0^{\pi/2} |\bar{E}_0|^2 \sin \theta d\theta + \int_0^{\pi/2} |\bar{E}_0|^2 \sin \theta \left[(2\pi J_0[2\theta]) \right. \right. \\ \left. \left. - \left(4\pi J_0[\sqrt{2}\theta] \right) \right] d\theta \right\}$$

Or

$$R_r = \frac{P}{30 I_0^2} \int_0^{\pi/2} \left\{ |\bar{E}_0|^2 \sin \theta \right\} \left\{ 1 + J_0(2ks \sin \theta) - 2J_0(\sqrt{2} ks \sin \theta) \right\} d\theta \quad (10)$$

This research is mainly concerned with corner reflectors illuminated by a center-fed linear dipole. (Other types of feed antennas will be considered in the next chapter.) The exciting current distribution on the dipole feed antenna is assumed sinusoidal, so that its far-zone field is given by⁷

$$\bar{E}_0 = \left[\frac{60 I_0}{R} \frac{\cos(kl/2 \cos \theta) - \cos kl/2}{\sin \theta} \right] \bar{i}_\theta \quad (11)$$

where: I_0 = peak value or amplitude of the current at an antinode, and

l = dipole length.

By substituting equation (11) in equation (10) and then using integral I_1 , page 11, there is obtained for the radiation resistance of the 90° corner reflector antenna with dipole feed

$$R_r = 60 I_1 + 120 \int_0^{\pi/2} \left[\frac{\cos(kl/2 \cos \theta)}{\sin \theta} \right]^2 \left[J_0(2ks \sin \theta) - 2J_0(\sqrt{2}ks \sin \theta) \right] d\theta$$

On page 49 of Appendix A it is explained that the quantity $60I_1$ is the (free-space) radiation resistance, R_{r_0} , of a center-fed dipole referred to an antinodal value of current, so that, referred to this current on the dipole feed antenna

$$R_r = R_{r_0} + 120 \int_0^{\pi/2} \frac{[\cos(kl/2 \cos \theta) - \cos kl/2]^2}{\sin \theta} \left[J_0(2ks \sin \theta) - 2J_0(\sqrt{2}ks \sin \theta) \right] d\theta \quad (12)$$

3.3B Radiation Resistance of 60° Corner Reflector Antennas

Substituting in the radiation resistance integral the summation in equation (3), expanding and squaring, and using the identity $\sin^2 B = 1/2 - 1/2 \cos 2B$ give

$$R_r = \frac{R^2}{90\pi I_0^2} \int_0^{\pi/2} \int_0^{2\pi} \left\{ \left| \bar{E}_0 \right|^2 \sin \theta \right\} \left\{ \left\{ 3/2 - 1/2 \left[\cos[2\theta \cos \phi] + \cos[2\theta \cos(\phi - \pi/3)] + \cos[2\theta \cos(\phi - 2\pi/3)] \right] \right. \right. \\ \left. \left. + 2 \left[\sin[\theta \cos \phi] \sin[\theta \cos(\phi - 2\pi/3)] - \sin[\theta \cos \phi] \sin[\theta \cos(\phi - \pi/3)] - \sin[\theta \cos(\phi - \pi/3)] \sin[\theta \cos(\phi - 2\pi/3)] \right] \right\} \right\} d\phi d\theta$$

Using integrals I_2 and I_3 , one obtains

$$R_r = \frac{R^2}{90\pi I_0^2} \int_0^{\pi/2} \left\{ \left| \bar{E}_0 \right|^2 \sin \theta \right\} \left\{ 2\pi \right\} \left\{ 3/2 + \left[J_0(\sqrt{3}\theta) - J_0(\theta) \right] - \left[J_0(\theta) - J_0(\sqrt{3}\theta) \right] - \left[J_0(\theta) - J_0(\sqrt{3}\theta) \right] - 3/2 \left[J_0(2\theta) \right] \right\} d\theta \\ R_r = \frac{R^2}{30I_0^2} \int_0^{\pi/2} \left[\left| \bar{E}_0 \right|^2 \sin \theta \right] \left[1 + \left\{ 2 \left[J_0(\sqrt{3}\theta) - J_0(\theta) \right] - J_0(2\theta) \right\} \right] d\theta \quad (13)$$

After substituting equation 11, page 13, for \bar{E}_0 , and then using $60 I_1 = R_{r_0}$ there is obtained for the 60° corner reflector antenna with dipole feed

$$R_r = R_{r_0} + 120 \int_0^{\pi/2} \left\{ \frac{[\cos(kl/2 \cos \theta) - \cos kl/2]^2}{\sin \theta} \right\} \left\{ 2 \left[J_0(\sqrt{3}ks \sin \theta) - J_0(ks \sin \theta) \right] - J_0(2ks \sin \theta) \right\} d\theta \quad (14)$$

3.30 Radiation Resistance of 45° Corner Reflector Antennas

Upon substitution in the radiation resistance integral the summation in equation (2), page 7, expanding and squaring, and using the identity $\cos B = 1/2 + 1/2 \cos 2B$, the following expression is obtained for the radiation resistance of 45° corner reflector antennas

$$R_r = \frac{R^2}{120\pi I_0^2} \int_0^{\pi/2} \int_0^{2\pi} \left\{ |\bar{E}_d|^2 \sin \theta \right\} \left\{ \left\{ 2 + 1/2 \left(\cos [2\theta \cos \phi] + \cos [2\theta \cos(\phi - \pi/2)] \right) \right. \right. \\ + \cos [2\theta \cos(\phi - \pi/4)] + \cos [2\theta \cos(\phi - \frac{3\pi}{4})] \Big\} \\ + 2 \left\{ \cos [\theta \cos \phi] \cos [\theta \cos(\phi - \pi/2)] - \cos [\theta \cos \phi] \cos [\theta \cos(\phi - \frac{\pi}{4})] \right. \\ + \cos [\theta \cos(\phi - \frac{\pi}{4})] \cos [\theta \cos(\phi - \frac{3\pi}{4})] - \cos [\theta \cos(\phi - \frac{\pi}{2})] \cos [\theta \cos(\phi - \frac{3\pi}{4})] \\ - \cos [\theta \cos(\phi - \frac{\pi}{2})] \cos [\theta \cos(\phi - \frac{\pi}{4})] \\ \left. \left. - \cos [\theta \cos \phi] \cos [\theta \cos(\phi - \frac{3\pi}{4})] \right\} \right\} d\phi d\theta$$

Through use of integrals I_2 and I_4 , one obtains

$$R_r = \frac{R^2}{120\pi I_0^2} \int_0^{\pi/2} \left\{ |\bar{E}_d|^2 \sin \theta \right\} \left\{ \left\{ 4\pi + (4\pi J_0(2\theta)) \right\} + 2\pi \left\{ \left[J_0(2\theta \sin \frac{\pi}{4}) \right. \right. \right. \\ + J_0(2\theta \cos \frac{\pi}{4}) \Big] - \left[J_0(2\theta \sin \frac{\pi}{8}) + J_0(2\theta \cos \frac{\pi}{8}) \right] \\ + \left[J_0(2\theta \sin \frac{\pi}{4}) + J_0(2\theta \cos \frac{\pi}{4}) \right] - \left[J_0(2\theta \sin \frac{\pi}{8}) + J_0(2\theta \cos \frac{\pi}{8}) \right] \\ \left. \left. - \left[J_0(2\theta \sin \frac{\pi}{8}) + J_0(2\theta \cos \frac{\pi}{8}) \right] - \left[J_0(2\theta \sin \frac{3\pi}{8}) + J_0(2\theta \cos \frac{3\pi}{8}) \right] \right\} \right\} d\theta \\ R_r = \frac{R^2}{120\pi I_0^2} \int_0^{\pi/2} \left\{ |\bar{E}_d|^2 \sin \theta \right\} \left[4\pi + 4\pi J_0(2\theta) \right. \\ \left. + 8\pi \left\{ J_0(\sqrt{2}\theta) - J_0(2\theta \sin \frac{\pi}{8}) - J_0(2\theta \cos \frac{\pi}{8}) \right\} \right] d\theta$$

Or

$$R = \frac{R^2}{30I_0^2} \int_0^{\pi/2} [|\bar{E}_0|^2 \sin \theta] \left[1 + \left\{ J_0(2\theta) + 2 [J_0(\sqrt{2}\theta) - J_0(0.7654\theta) - J_0(1.8478\theta)] \right\} \right] d\theta \quad (15)$$

Proceeding as was done previously on page 15, there is obtained for the dipole-fed 45° corner reflector antenna

$$R_r = R_{I_0} + 120 \int_0^{\pi/2} \left\{ \frac{[\cos(kl/2 \cos \theta) - \cos kl/2]^2}{\sin \theta} \right\} \left\{ J_0(2ks \sin \theta) + 2 [J_0(\sqrt{2} ks \sin \theta) - J_0(0.7654 ks \sin \theta) - J_0(1.8478 ks \sin \theta)] \right\} d\theta \quad (16)$$

3.3D Radiation Resistance of Other Corner Reflector Antennas

The radiation resistance of corner reflector antennas for which $m = 10, 14, 16, 18 \dots$ may be obtained in precisely the same fashion as used above for the cases $m = 4, 6$, and 8 . Substituting in the radiation resistance integral the summation in either equation 2 or equation 3, and expanding and squaring will introduce in the integrand only terms of the form given below:

$$A_b^a = \frac{\cos^2}{\sin^2} \left\{ \left[ks \sin \theta \right] \left[\cos \left(\frac{2\pi p}{m} - \phi \right) \right] \right\}$$

$$B_b^a = \frac{\cos}{\sin} \left\{ \left[ks \sin \theta \right] \left[\cos \left(\frac{2\pi p}{m} - \phi \right) \right] \right\} \times \frac{\cos}{\sin} \left\{ \left[ks \sin \theta \right] \left[\cos \left(\frac{2\pi q}{m} - \phi \right) \right] \right\}$$

Using $\cos^2 B = 1/2 + 1/2 \cos 2B$ for the terms given in A_a , and $\sin^2 B = 1/2 - 1/2 \cos 2B$ for the terms given in A_b , will yield

$$A_b^a = 1/2 \pm 1/2 \cos \left\{ \left[2 ks \sin \theta \right] \left[\cos \left(\frac{2\pi p}{m} - \phi \right) \right] \right\}$$

These parts of the integrand may be integrated by using integral I_2 . The terms of the form given in B_a and B_b , above may be integrated by using integrals I_4 and I_3 , respectively. Consequently, the radiation resistance integral may be integrated (with respect to ϕ) for every value of m , and therefore, for every corner angle α . It is to be noted that the above discussion is valid for corner reflectors illuminated by any type of feed antenna excited uniformly with ϕ . In the next chapter more will be said regarding the latter subject.

3.4 Numerical Evaluation of Radiation Resistance and Antenna Gain

Equations 12, 14, and 16, pages 13, 14, and 16, were shown to equal the radiation resistances of 90° , 60° , and 45° corner reflector antennas fed by linear dipoles. Considerable effort was spent in trying to integrate analytically the integrals contained in those equations but all attempts proved unsuccessful. It was therefore necessary to employ a numerical method of integration.

From the equations referred to, it is seen that the radiation resistance for each of the cases $\alpha = 90^\circ$, 60° , and 45° , or $m = 4$, 6, and 8, may conveniently be represented by R_r as given in the equation

$$R_r \equiv R_{r_0} + 120 I_m = R_{r_0} + R_1 \quad (17)$$

where I_m = the integral in equation 12, 14, or 16. Values of R_r were obtained from values of R_{r_0} and I_m determined as follows:

Simpson's rule was employed for numerical integrations of I_m ; required values of the first order Bessel function were obtained from reference No. 8 of the Bibliography. And R_{r_0} was computed from the solution of integral I_1 (See page 10 or page 49 of Appendix A) using values of the sine integral, the cosine integral, and the natural logarithm given in reference No. 9.

Antenna gains in the direction $\theta = 90^\circ$, $\phi = 0^\circ$ (the forward direction) were determined using the equation

$$G(90^\circ, 0^\circ) = \frac{480}{R_r} [1 - \cos kl/2]^2 r^2 (s, 90^\circ, 0^\circ)$$

which is equation 9 of page 10 with \bar{E}_0 set equal to the free space field of the dipole feed antenna of length l .

The quantities R_r and $G(90^\circ, 0^\circ)$ were calculated as functions of frequency in the two to one frequency band $0.8 f_0 \leq f \leq 1.6 f_0$ for corner to dipole spacings (s) of $\lambda_0/4$, $\lambda_0/2$, $3\lambda_0/4$, and λ_0 , where the significance of λ_0 and f_0 is as defined by the identity $\lambda_0 = 2l$. These calculations were made for frequency ordinates of $0.8 f_0$, $0.9 f_0$, $1.0 f_0$. . . $1.6 f_0$, so that nine values of the functions R_r and $G(90^\circ, 0^\circ)$ were obtained for each setting of α and s considered.

The results, including the dipole radiation resistance R_{T_0} , are plotted in Figs. 6 - 9, inclusive. It is seen that the 800 to 1600 mc band is used for the curves; this frequency band was chosen so as to conform with frequencies of interest in the experimental measurements remaining to be described. (But the length of the dipole feed can be modeled to suit any λ_0 so that the curves are valid for every frequency band $0.8 f_0 \leq f \leq 1.6 f_0$.)

Examination of the curves shows that very favorable gain characteristics, constancy of gain for two to one frequency band, are predicted for the corner reflector antennas defined by $\alpha = 90^\circ$, $s = \lambda_0/4$; $\alpha = 90^\circ$, $s = \lambda_0/2$; $\alpha = 60^\circ$, $s = \lambda_0/2$; and $\alpha = 45^\circ$, $s = \lambda_0/2$. Theoretical basis for selecting any of these antennas for development as a gain standard is clearly established.

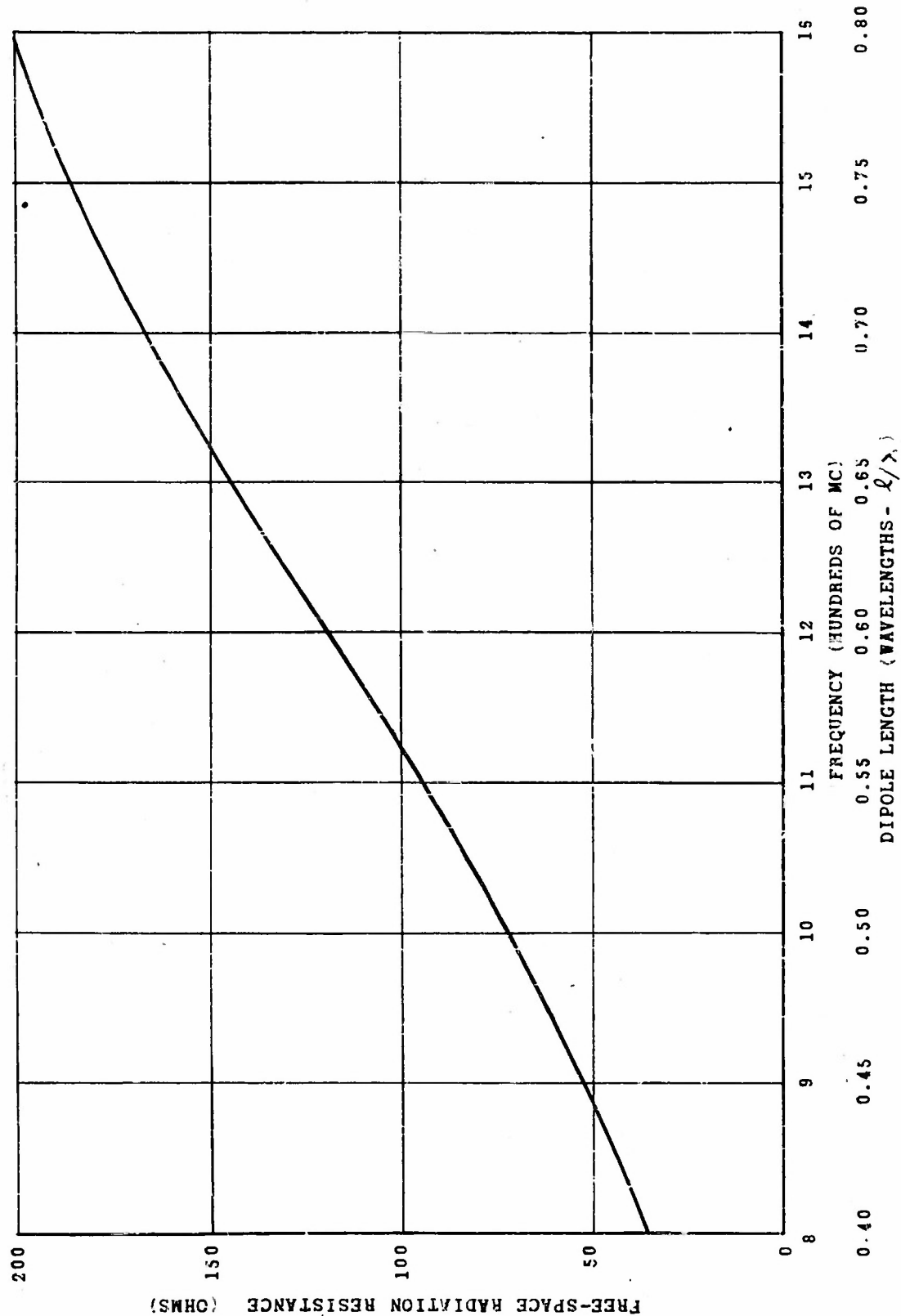


FIG. 6 LINEAR DIPOLE RADIATION RESISTANCE vs DIPOLE LENGTH

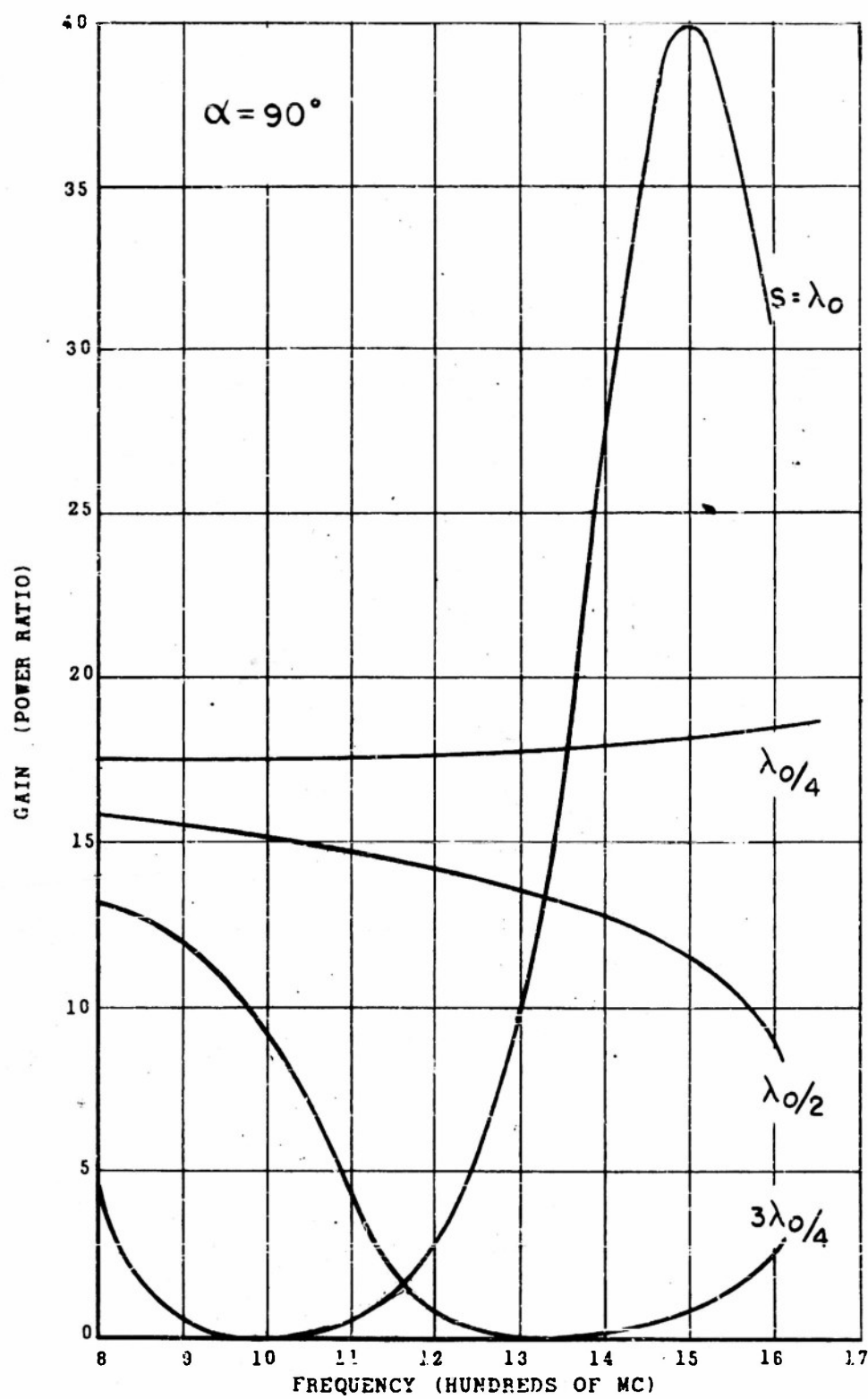


FIG. 7A CALCULATED GAIN vs FREQUENCY

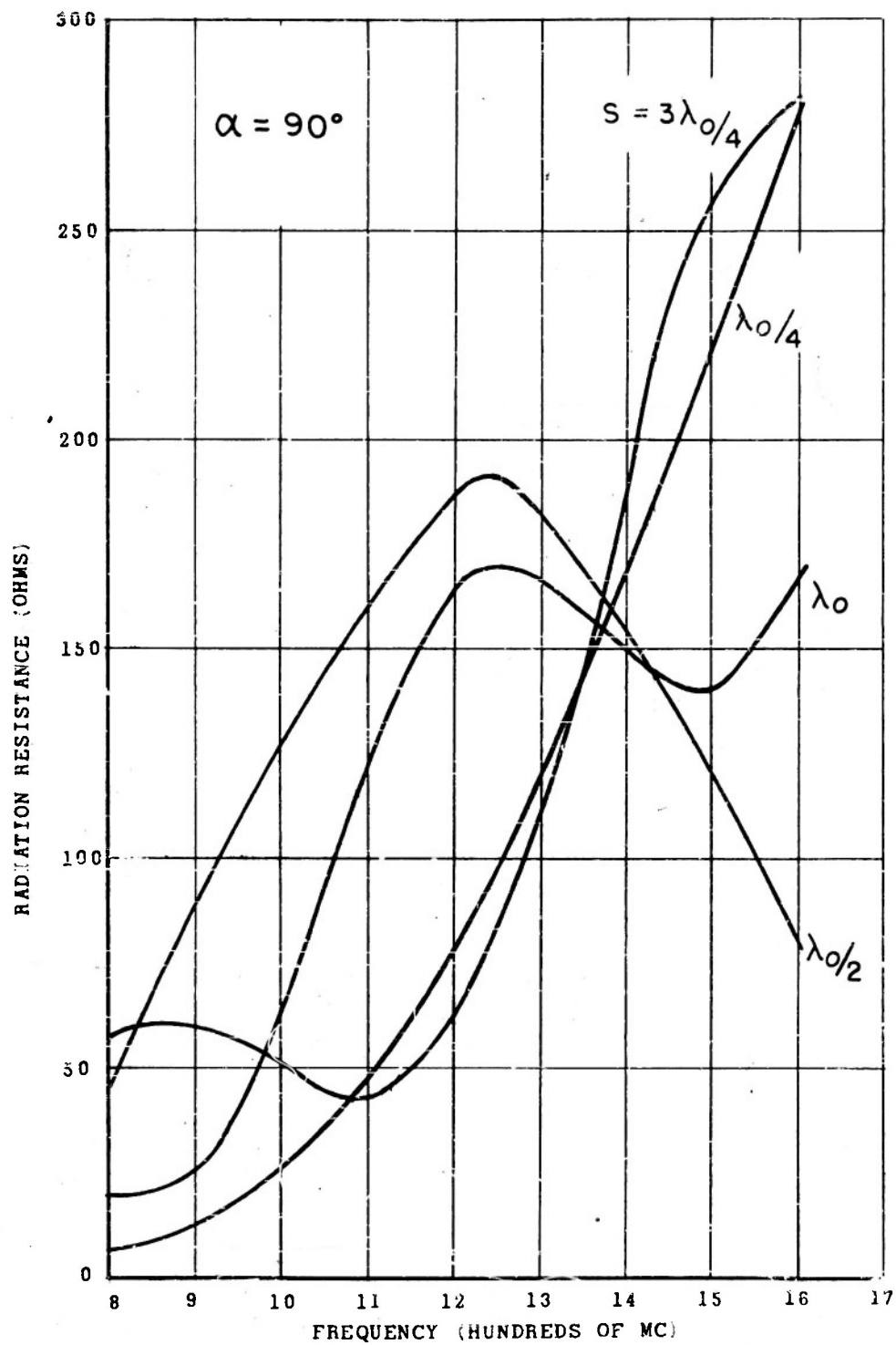


FIG. 7B CALCULATED RADIATION RESISTANCE vs FREQUENCY

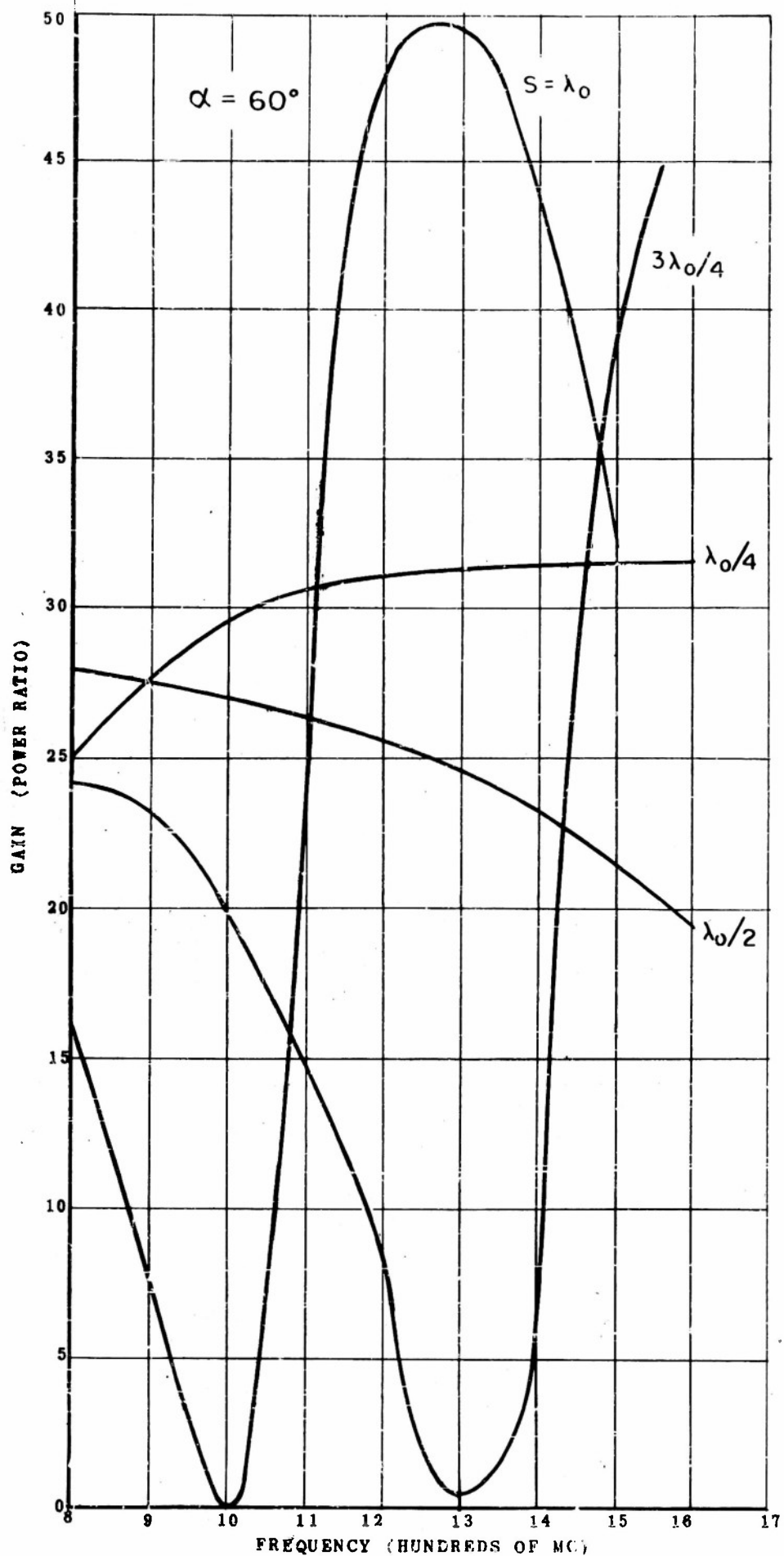


FIG. 3A CALCULATED GAIN RESISTANCE vs FREQUENCY 19D

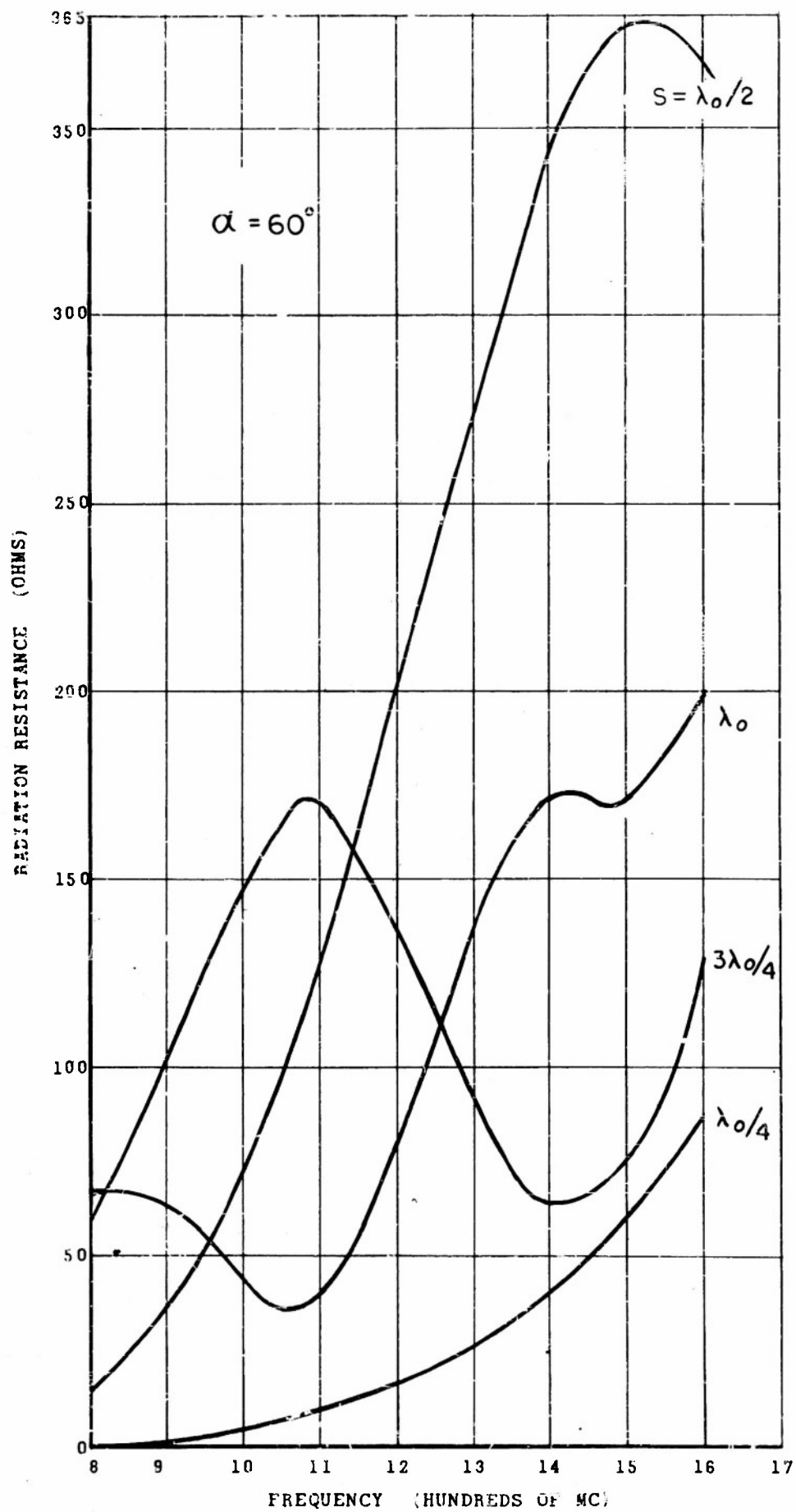


FIG. 8B CALCULATED RADIATION RESISTANCE vs FREQUENCY

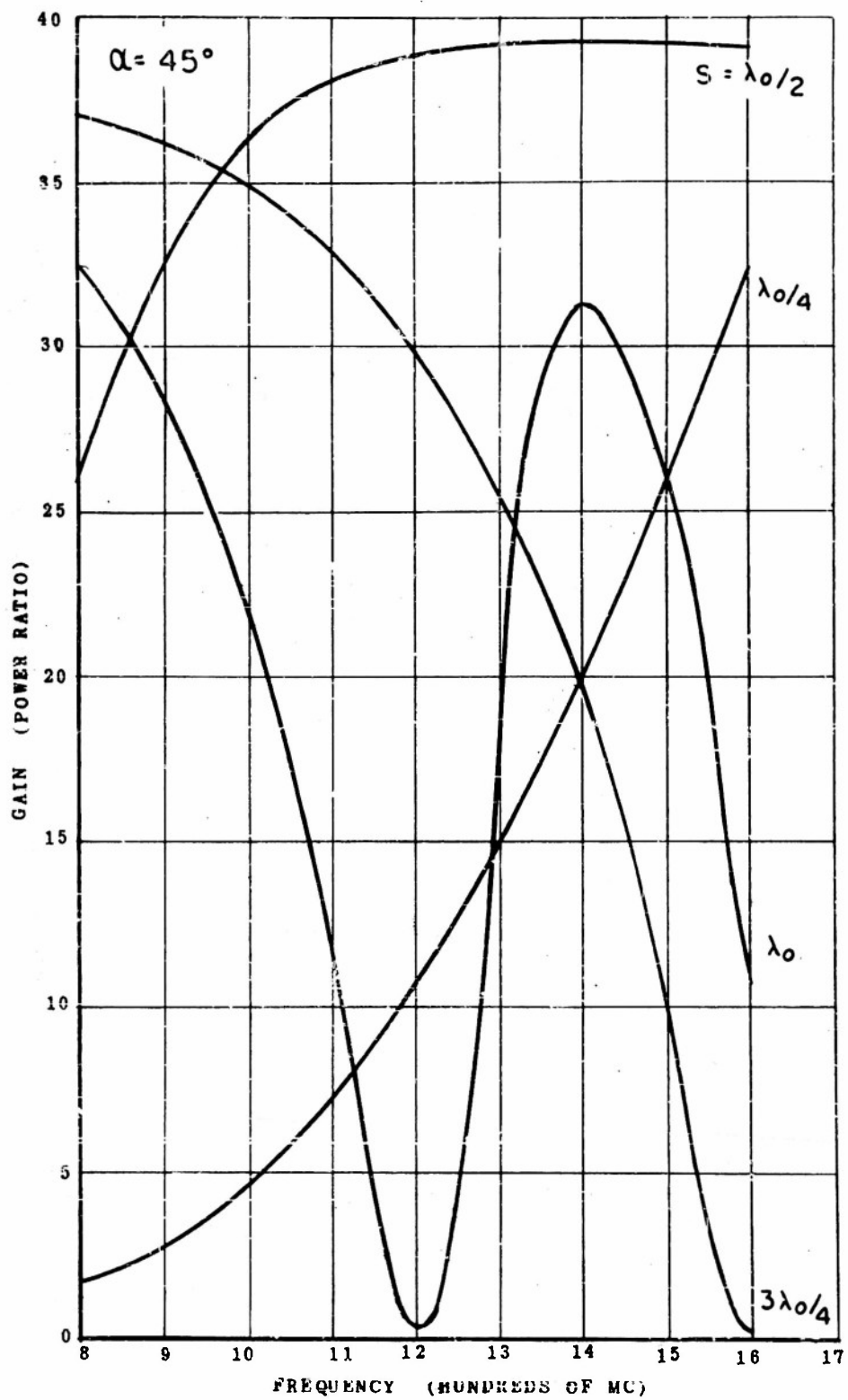


FIG. 9A CALCULATED GAIN vs FREQUENCY

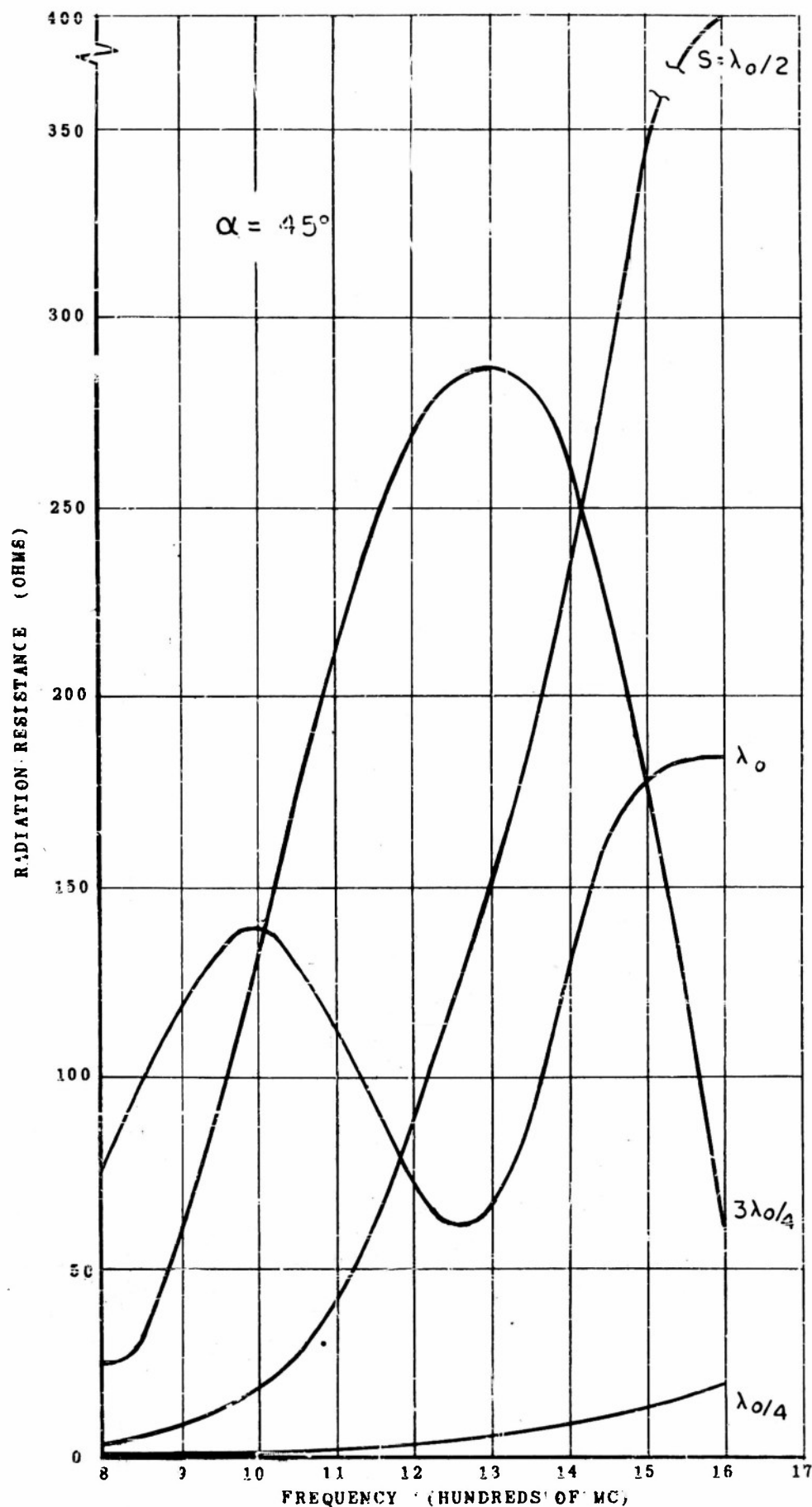


FIG.9B CALCULATED RADIATION RESISTANCE vs FREQUENCY

3.5 Accuracy of the Calculations

Radiation resistances and antenna gains were computed for 108 individual cases. Several precautions were taken in order to ensure accuracy. Values of sine integral, cosine integral, logarithmic, and trigonometric functions accurate to four decimal places, and values of the zero order Bessel function accurate to at least three decimal places were used. Multiplication and division were made using a Friden model ST automatic calculator.

Preliminary tests of the convergence of the numerical integrations of I_m were made and will now be explained. Sub-intervals of 9° , $7\frac{1}{2}^\circ$, and 5° were used in Simpson's rule and answers to I_m were computed for five of the 108 cases. In four of these five test-computations, the answers obtained using $7\frac{1}{2}^\circ$ sub-intervals were different in the third decimal place from those obtained using 9° sub-intervals. Improvement in the third decimal place was noted for the remaining case when the results of the third set of computations -- those obtained using 5° sub-intervals -- were compared with the results of the second set. Therefore, it may be concluded that all of the five answers of the third set of computations were determined accurate to at least three decimal places.

A small percentage increase in accuracy to be obtained if a sub-interval smaller than 5° were used in the many integrations to follow was not believed worth the considerably larger percentage increase in time that would be spent operating the calculator. Consequently, it was decided to use 5° sub-intervals for the (103) integrations remaining.

It should be pointed out that in some values of radiation resistance errors of about one-half ohm are believed possible. The dipole radiation resistance, R_{r_0} , definitely was calculated accurate to at least three decimal places. But the favorable conclusion from the five sample integrations of the above described convergence tests does not prove conclusively that no error in the third decimal place of the other 103 integrations was obtained. For any one of these integrations of I_m it is believed that .004 ohm (ΔI_m) is a safe estimate of maximum error; therefore,

$$\Delta R_r = \Delta (R_{r_0} + 120 I_m) < 121 \Delta I_m \approx 0.5 \text{ ohm.}$$

Now, in cases where R_r is less than ten ohms an error of one-half is greater than five percent. But fortunately, a big majority of the values are larger than ten ohms. In fact, 78 percent are larger than 25 ohms, and the error in these values is probably less than two percent. Of course, the error in corresponding values of gain is also less than two percent, or 0.09 db.

The writer's research supervisor agreed that recomputing the low radiation resistances (using a smaller sub-interval in Simpson's rule and/or more significant figures) was not merited inasmuch as these values of radiation resistance are not of practical importance: antennas having low radiation resistances are very seldom used because loss resistance may be of the same order of magnitude as radiation resistance.

Kraus computed the radiation resistance of dipole-fed corner reflector antennas using a method^{*} entirely different from the Poynting vector method used herein. Kraus considered only the case wherein the length of the dipole is exactly a half wavelength. A check between the values given on the curves in this report (for the one case $\lambda = \lambda_0$, $f = f_0 = 1000$ mc.) and those computed by Kraus is as shown in Table I. The latter values are designated by R_r' and were read accurate to approximately one-half ohm from the curves in reference 10 a.

TABLE I

	s	R_r (Ohms)	R_r' (Ohms)
90°	0.25 λ	27.3	27
	0.5 λ	127	126
60°	0.25 λ	2.83	4
	0.5 λ	71.4	72

It is seen that, percentagewise, the check between the results is very good with the exception of those for the case $\alpha = 60^\circ$, $s = 0.25 \lambda$. This circumstance led the writer to calculate the radiation resistance for the case in question by the method used by Kraus. A value of 2.739 ohms

*To be considered on page 23

was obtained. Accordingly, it is surmised that either Kraus made an error in calculating his answer, or else the curve from which the answer was taken is printed in error in the immediate region of $R_x' = 4$ ohms.

IV. THE POYNTING VECTOR METHOD VS. THE CIRCUIT METHOD

Analytical investigations on corner reflector antennas predating the investigation made herein use a method which might be called the "circuit method". Briefly, the dipole feed antenna and its images are considered as a system of mutually coupled circuits and the radiation resistance of the corner reflector antenna (or of an antenna array) is obtained therefrom using ordinary circuit theory.^{4, 10a, 11, 13} This circuit method requires calculation of the "self resistance" of the dipole and the mutual resistances between the dipole and its images. (See Appendix B.) Since the Poynting vector method was used in this report, some explanation may be in order.

Let it first be said that the writer personally prefers the Poynting vector method for analysis of all types of antennas. A second reason for selecting the Poynting vector method is that the study described herein was meant to be an original research, so that using the new approach to the corner reflector problem was justified on that basis alone. Certain real advantages favoring the Poynting vector method over the circuit method became evident at various intervals during this research and these advantages should be pointed out.

At the beginning, calculations were made using the circuit method. The expressions giving the self resistance and mutual resistance are very lengthy, and they were found exceedingly cumbersome to work with unless the length of the dipole feed antenna is exactly an odd number of half wavelengths.* This circumstance caused the writer to explore the possibilities of the Poynting vector method, and the double integrals which were determined could be integrated analytically only once. Nevertheless, it was found that in one computation of radiation resistance by each method -- with $l \neq \lambda/2$ -- a moderate, yet appreciable, saving of time was gained by the new method. A moderate saving of time in one computation multiplied by the large number of computations to be made amounted to a large saving in the total time spent operating the calculating machine. (This advantage removed any doubts as to which method of calculation would be used.)

Another advantage that was gained and is believed of importance will

*The above statement will be appreciated by noting the length, and the complexity, of Equation B.4 of Appendix B. This equation multiplied by 120 equals the sum of the mutual resistances for the case $\alpha = 90^\circ$; this sum must be added to R_{r0} to obtain R_r . Corresponding equations for $\alpha = 60^\circ$ and $\alpha = 45^\circ$ are about $1\frac{1}{2}$ and 2 times as long as Equation B.4.

now be explained. It is clear that equations (10), (13), and (15) of chapter III give the radiation resistances of all 90° , 60° , and 45° corner reflector antennas so long as \bar{E}_0 , the field of the feed antenna, is a function only of theta. Such a field will obviously be radiated by any source excited uniformly with azimuth angle, ϕ .

Now, of course, the integrals in the above equations can be solved numerically for any $\bar{E}_0(\theta)$ in the same manner as was used for the case $\bar{E}_0(\theta) = E_0(\theta)_d$, the subscript d denoting a dipole. In regard to these future calculations, it is estimated that at least half of the numerical data that would be required has already been computed, as will now be explained. It is seen that each of the equations (10), (13), and (15) may be written as follows:

$$R_r = \frac{R^2}{30 I_0^2} \int_0^{\pi/2} \left[|\bar{E}_0(\theta)|^2 \sin \theta \right] \left[1 + U_m(\theta) \right] d\theta \quad (18)$$

where $U_m(\theta)$ is in no way dependent on the type of feed antenna. For the case of the dipole feed, equation (18) was transformed to the form

$$R_r = \frac{R^2}{30 I_0^2} \int_0^{\pi/2} |\bar{E}_0(\theta)_d|^2 \sin \theta d\theta + \frac{R^2}{30 I_0^2} \int_0^{\pi/2} |\bar{E}_0(\theta)_d|^2 \sin \theta U_m(\theta) d\theta \quad (19)$$

$$R_r = R_{r_0} + 120 I_m$$

Now, $U_m(0^\circ)$, $U_m(5^\circ)$, $U_m(10^\circ)$. . . $U_m(90^\circ)$, the expressions containing the Bessel functions, were necessarily evaluated in order to determine the 108 answers of I_m . From this fact and from (18), it should be clear that the second statement of this paragraph, and the advantage implied, have been verified. Two possible corner-reflector feed antennas for which this advantage is applicable are a spherical dipole and a biconical horn; these feeds can be excited uniformly in azimuth, which is here required.

In computing the radiation resistance of the dipole-fed corner reflector, equation (18) was changed to equation (19) because the self resistance had already been calculated, as a function of frequency, when the circuit method was tried. Consequently, the simple expediency of multiplying values of self resistance by $2 \sin^2 K/2$ to obtain* the dipole radiation resistance, R_{r0} , was in evidence. Not only was the future numerical work shortened, but also, it was thereby possible to supplement this report with the curve of the function R_{r0} . In other calculations, it will be more expedient to solve numerically the entire integral of equation (18) in which case the radiation resistance of the feed antenna evidently will not be determined.

It should be emphasized that no advantage comparable to the one described would have been gained had the circuit method been used. At present, analytical expressions for self and mutual resistances have been derived only for the linear dipole antenna. To derive corresponding expressions for other types of feed antennas first requires the derivation of their near-zone fields. (In fact, the field just outside the surface of the feed antenna due to its own current is required to compute self resistance and the field at the same place due to the current in an image antenna is required to compute mutual resistance.^{10b, 11}) Now, the near-zone fields are considerably more difficult to determine than the far-zone fields required in the Poynting vector method. Even if the expressions for self and mutual resistance are derivable, it is unlikely that they would be very similar to those for the linear dipole. Therefore, calculations of corner reflector radiation resistance and antenna gain "simultaneously valid" for several differently illuminated corner reflectors, most likely, are not possible from the circuit method of analysis.

*As explained on page 49 of Appendix A

V DESIGN OF THE CORNER REFLECTOR ANTENNAS

5.1 Factors in the Design

Factors which required consideration in the design of the corner reflector antennas used in the experimental investigations to be described are the following:

- (1) Total cost of construction
- (2) Flexibility of design so as to permit the setting of several combinations of antenna parameters.
- (3) Size and weight
- (4) Agreement between measured and calculated radiation patterns and antenna gains.

A logical solution to the design problem was made apparent by combined consideration of (1) and (2): it would be advantageous to construct a single corner reflector assembly having features which permit wide variations of corner angle and feed antenna to corner spacing. In this way, a large number of distinct corner reflector antennas would be attainable for a comparatively low total cost. Therefore, it was decided to design a "variable" corner reflector antenna.

Factors (3) and (4) remained to be considered. The variable corner reflector antenna need be of moderate size and weight to facilitate mounting and transporting. On the other hand, calculated radiation pattern and gain are strictly valid only for infinite corner reflectors. Moreover, for a finite corner reflector antenna — in contrast to the infinite corner reflector — as the corner angle (α) is decreased from 90° , a steady increase in gain can not be expected. This fact is readily verified in the next paragraph.

The gain of any antenna is given by the well known equation $G = 4\pi fA/\lambda^2$, where A is the area of the antenna aperture and f is the illumination efficiency, which approaches unity for a matched antenna as its aperture is illuminated more and more uniformly. Now, the aperture area of a corner reflector antenna is closely approximated by the equation $A(\alpha) = 2hd \sin \alpha / 2$ where h and d are the horizontal and vertical dimensions of the reflector planes. For constant frequency, therefore, $G(\alpha) \sim f(\alpha) \sin \alpha / 2$ so that the gain will increase as α is decreased from 90° provided that the illumination efficiency increases sufficiently. But unless $f(90^\circ)$ is appreciably smaller than unity to begin with, decreasing gain will soon be the result.

The discussion of the preceding paragraph obviously discourages the use of corner reflectors having corner angles much smaller than 90° . Nevertheless, the variable corner reflector antenna was constructed. Reflector dimensions were made larger than recommended minimum values for the design of a 90° corner reflector in hopes that satisfactory correlation between computed and measured performance might be obtained at least for some corner to feed antenna spacings with $\alpha = 60^\circ$. In regard to a 90° corner reflector, Kraus^{10c} suggests that a practical design rule is to make the side length (h) at least twice the corner to feed antenna spacing. In addition, Kraus states that requirements on the depth (d) of the reflector are not critical, a depth equal to $1\frac{1}{2}$ times the length of the feed antenna being sufficient. Dimensions chosen for the variable corner reflector are $d = 11"$ and $h = 15"$. The latter dimension is greater than twice the largest corner to feed antenna spacing, s, that was expected to be used in the experimental measurements and about four times as large as the settings of s expected to be most often used.

5.2 Design Features of the Variable Corner Reflector

Engineering drawings of Fig. 24, attached at the end of the Report, and the photograph on the next page and that on page 31A show the essential features of the variable corner reflector. Two lengths of piano hinge fasten together the two reflector frames, permitting the corner angle to be varied from 10° to 105° . The purpose of the "variable braces", located at the top and bottom of the assembly (see Drawing No. 2), is to provide support for holding the reflector planes at any corner angle setting. The "dipole supporting brace" (Drawings No. 4 and No. 5), supports the feed antenna and its transmission line. The feed antenna may be moved to any distance from the corner by pulling on the brass tubing transmission line. This tubing is fitted snugly to the various parts of the dipole supporting brace, but no difficulty in adjusting the feed antenna to a particular setting is encountered if a small amount of Lubriplate lubricant is spread on the brass tubing.

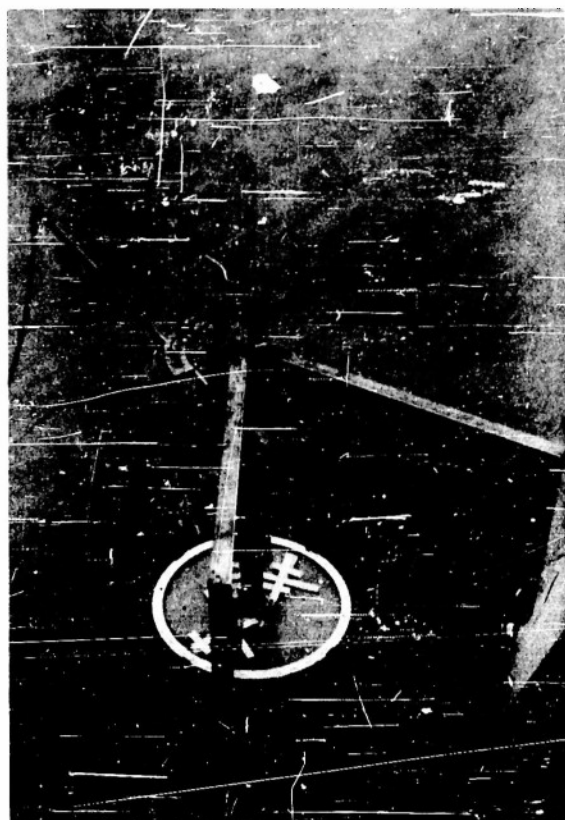


FIGURE 10
VARIABLE CORNER REFLECTOR ANTENNA

5.3 The Choice and the Design of the Feed Antenna

As already mentioned, comparison between calculated performance and measured performance was desired. For this reason and also because all qualitative analyses on corner reflector antennas assume that a linear dipole illuminates the reflector, that type of feed antenna was selected for the variable corner reflector antenna. (It is necessary to insert parenthetically that the variable corner reflector was designed and experimental measurements were started several months in advance of the starting date of the theoretical analysis of Chapter III. As was demonstrated, the analysis of Chapter III may be applied to corner reflectors having various types of feeds. This circumstance, of course, was not known when the feed antenna for the variable corner reflector was selected so that the possibility of using feeds other than linear dipoles was not considered.)

Fig. 11 on the next page shows the dipole feed antenna assembly in cross-section. The gap between the two sections of the dipole was made as small as is consistent with considerations of voltage arc-over and lumped capacitance. This gap need be small compared with wavelength, otherwise the length g of the inner conductor of the feed line will place inductance in series with the lower section of the dipole, resulting in unbalance between the currents in the dipole sections.

The short cylinder of lucite extending inside both brass tubings strengthens the construction and keeps the two dipole sections in alignment.

The necessity for including a balun in the design of the dipole feed antenna is apparent. In regard to baluns, it has been demonstrated^{2b} that a balun length (l_b) slightly less than the nominal $\lambda/4$ is optimum, and for several dipole systems, a balun 0.23 wavelength long was found by experiment to give good results. Accordingly, the shorting bar of the balun on the dipole feed assembly was set at 0.23λ in all the measurements to be described.

It is mentioned that the dipole feed assembly can be removed, undamaged, from the variable corner reflector. This will permit use of the variable corner reflector in future investigations using other types of feed antennas. From engineering drawing No. 6, it is clear that unsoldering the type-N connector on the far end of the feed line permits the entire dipole feed assembly to be pulled free from the dipole supporting brace. In addition, this brace is removed merely by tilting it to clear the grooves in the variable brace. Then, to com-

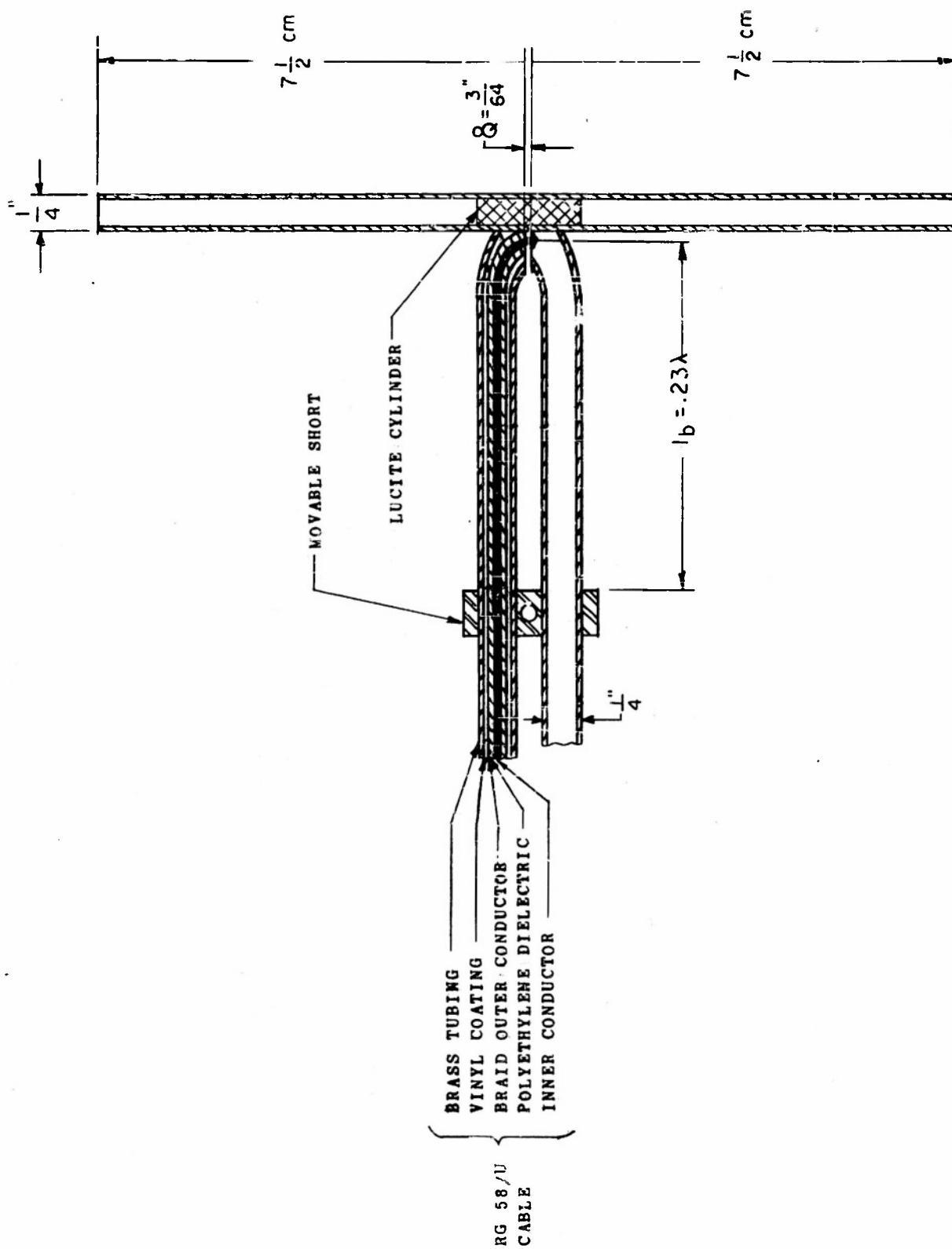


FIG. 11 DIEPOLE CROSSECTION

plete the modification, a "feed-antenna supporting brace" accommodating the new type of antenna feed can be inserted in these grooves.

VI TRANSMITTING AND RECEIVING EQUIPMENT

Transmitting equipment and receiving equipment used in all of the antenna measurements that will be described are shown in Figs. 12 and 13 on the next page (31A). An APT transmitter, having a cw power output of 5 - 10 watts, was connected to the transmitting antennas used, and received signals were amplified by an APR receiver and indicated on a dc milliammeter.

Incorporated in the APR receiver is a biased detector whose dc output was found to be only approximately proportional to the cw signal at the receiver input. Therefore, calibration of the receiver was necessary. This calibration was performed at every hundred mc in the 800 mc - 1600 mc band by employing an LAE signal generator for the calibration frequencies from 800 - 1300 mc and an LAF signal generator for the remainder of the band. The above signal generators each contain an accurately calibrated attenuator and wavemeter thereby permitting calibration of the receiver in the customary manner.

Transmitted frequencies were adjusted to 800 mc, 900 mc, 1000 mc . . . 1600 mc simply by carefully tuning the APT transmitter to the peak of the pass band of the calibrated APR receiver.

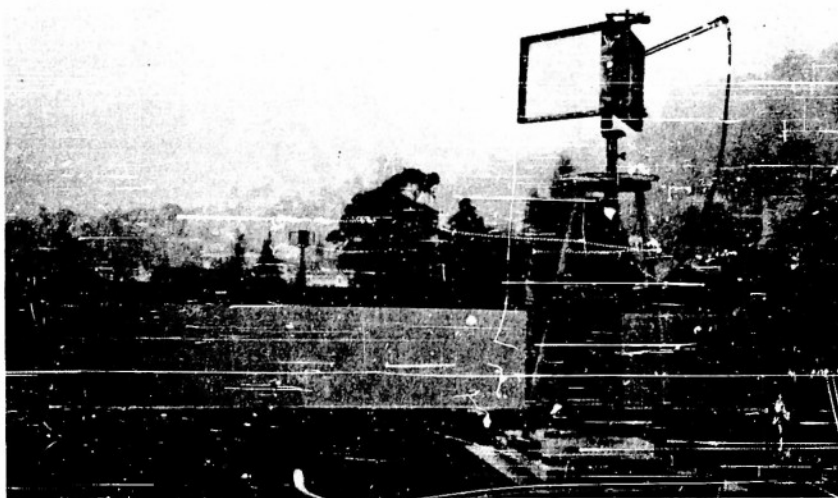


FIGURE 12

TESTING SITE FOR H-PLANE PATTERN MEASUREMENTS

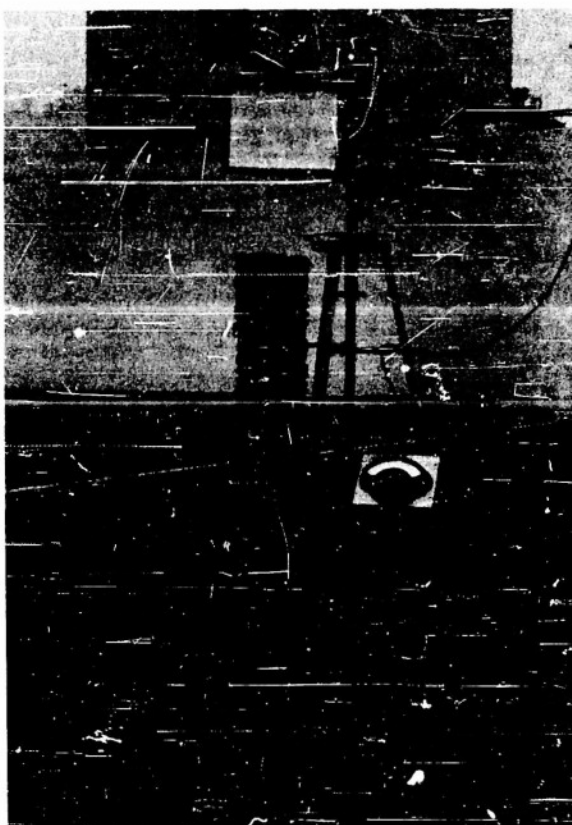


FIGURE 13

H-PLANE PATTERN MEASUREMENTS

VII PRELIMINARY MEASUREMENTS

H-plane radiation patterns of the variable corner reflector antenna for corner angles of 90° , 60° , and 45° were measured at a frequency of 1000 mc for corner to dipole spacings of $7.5 \text{ cm} = \lambda_0/4$, $15 \text{ cm} = \lambda_0/2$, $22.5 \text{ cm} = 3\lambda_0/4$, and $30 \text{ cm} = \lambda_0$. Each radiation pattern was measured twice for reasons made evident in the succeeding paragraph.

Measurements were first taken on the flat roof of a large building. These radiation patterns were appreciably broader than was expected and various jagged variations together with several minor lobes were present. It was suspected that reflections from the roof, and possibly from a distant three-foot guard rail around its periphery, were responsible for the unwanted results. Measurements were repeated which verified that suspicion.

The second measurements were taken at the testing site pictured in Fig. 12. The variable corner reflector antenna and a 90° corner reflector transmitting antenna were placed on opposite sides of a four-story air shaft --- centrally located, incidentally, in the building on which the previous measurements were taken --- so that only negligibly small ground-reflected signals were able to reach the receiving antenna. Reflections from an elevator tower protruding skyward on the far side of the air shaft were made quite small by directing the beam of the transmitting antenna away from this tower.

The transmission range (the width of the air shaft) was several times larger than $2d^2/\lambda$ so that phase variation across the receiving aperture was probably negligible. Moreover, it was found that in the vicinity of the receiving antenna the field intensity was uniform over an area of approximately three square feet, or nearly twice the area of the maximum receiving aperture used. From this paragraph, and the preceding one, it is apparent that ideal conditions were closely approximated at the testing site described.

The results of the second set of H-plane radiation pattern measurements are shown in Figs. 14 to 16, inclusive. Calculated patterns, obtained using either equation (2) or equation (3) with $\lambda = \lambda_0/2$ and $\theta = 90^\circ$, are included for comparison. In the case of $\alpha = 45^\circ$, results are shown only for a corner to dipole spacing of $s = \lambda_0/4$ (Fig. 16, page 330). Variation of s caused only minor change in the measured result. For this corner angle, the

measured patterns were much broader than corresponding calculated patterns and considerably broader than those measured for $\alpha = 90^\circ$ and $\alpha = 60^\circ$. Therefore, it may be concluded, from only these preliminary measurements, that the gain for $\alpha = 45^\circ$ is much smaller than that for both of the other corner angles.

The primary objective of the measurement of the above radiation patterns was to obtain a first indication of how well the performance of the variable corner reflector antenna agrees with calculated performance. As already inferred, for $\alpha = 45^\circ$ it was found that there is essentially no correlation between calculated and actual performances. This correlation is definitely improved for $\alpha = 60^\circ$, excepting the case $s = \lambda_0$, wherein the measured pattern does not consist of two main lobes as does the calculated. (It might be mentioned that increasing s to about $9/8 \lambda_0$, caused the appearance of two main lobes.) But the patterns for the 60° corner reflector are yet appreciably different from those calculated. Finally, for $\alpha = 90^\circ$ a very good correlation exists in the cases of $s = \lambda_0/4$ and $s = \lambda_0/2$, and a fair correlation in the case of $s = 3\lambda_0/4$; for a corner to dipole spacing of λ_0 , the measured and calculated patterns are compatible only insofar as the presence of two main lobes is concerned.

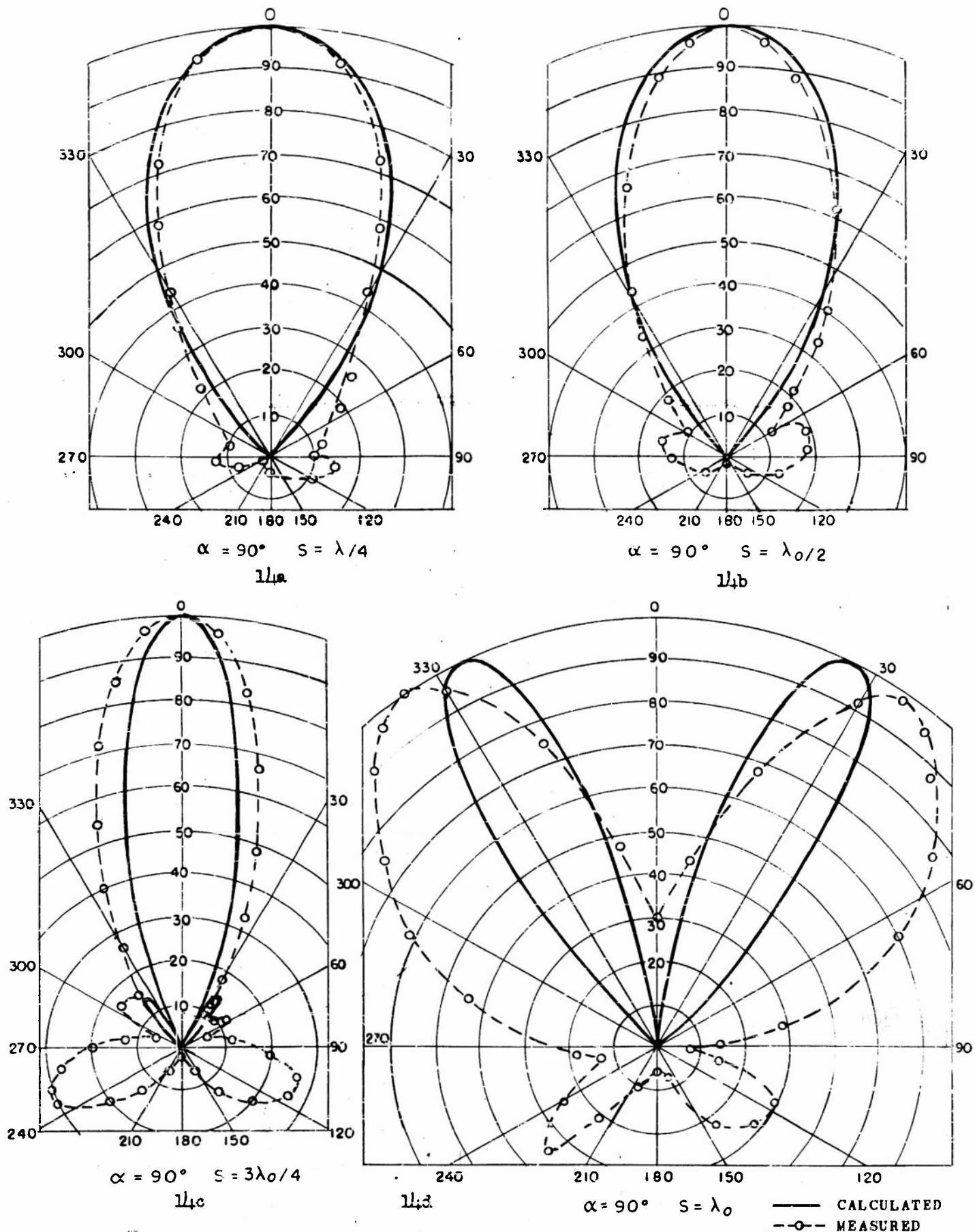


FIG. 11. MEASURED AND CALCULATED H-PLANE ELECTRIC FIELDS
FOR CORNER REFLECTOR ANTENNA

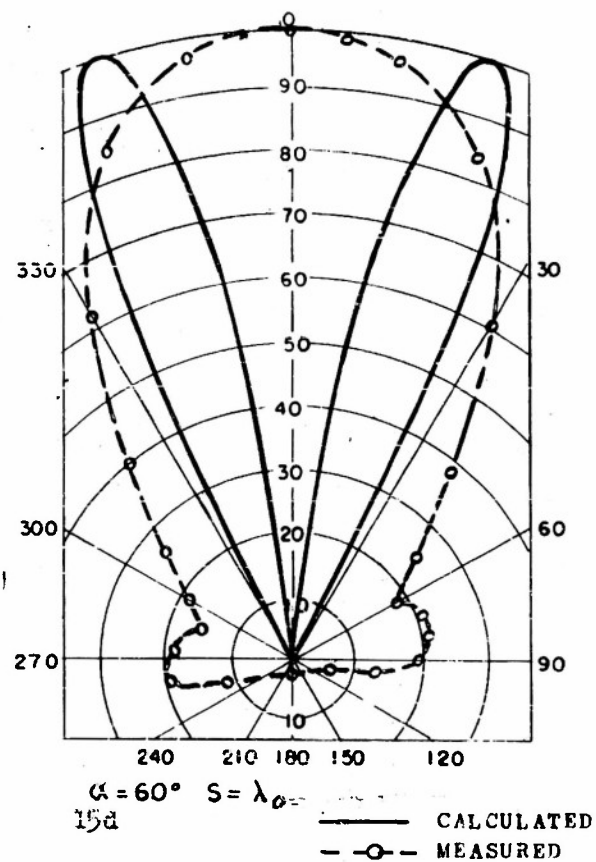
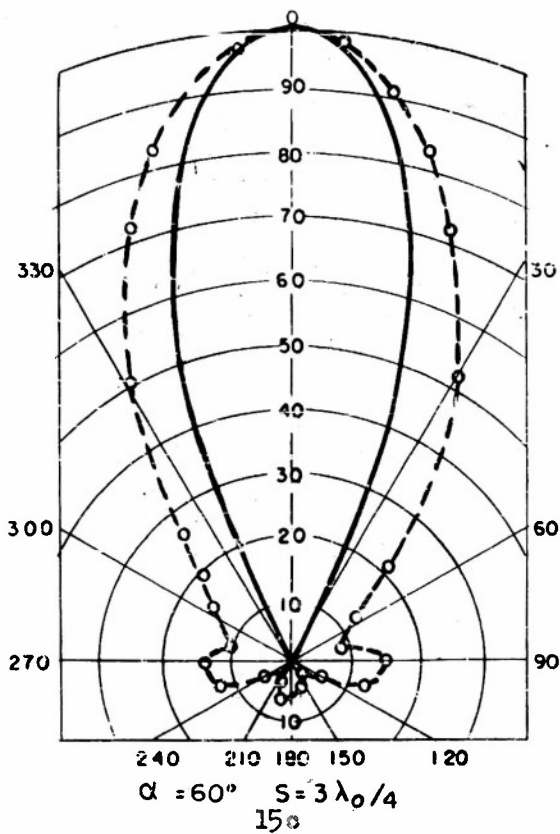
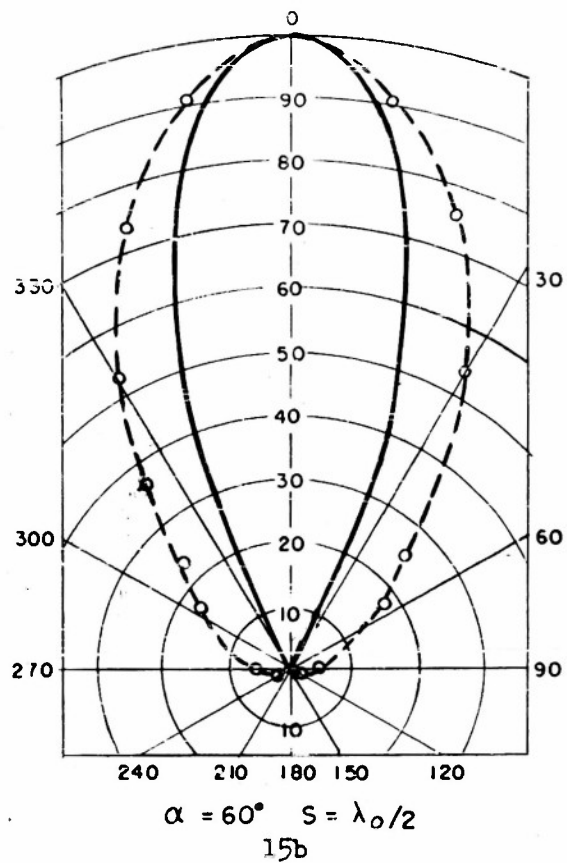
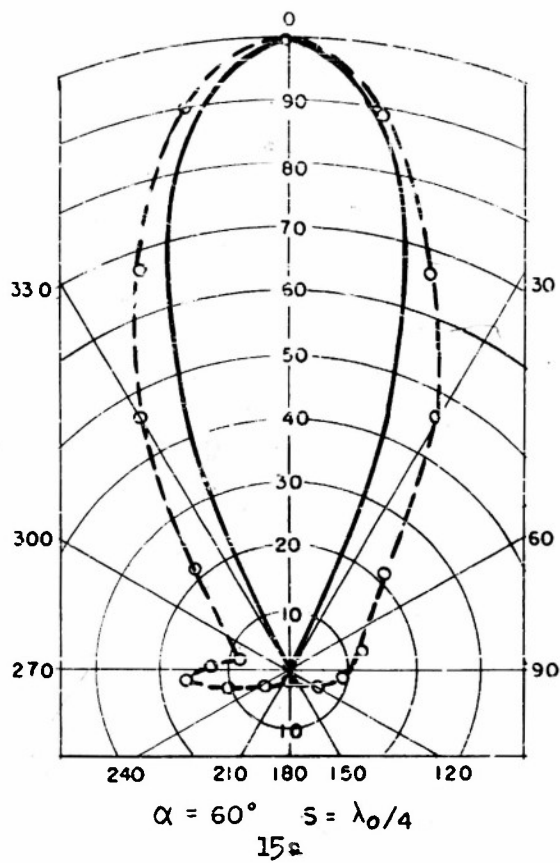


FIG. 15 MEASURED AND CALCULATED H-PLANE ELECTRIC FIELD
FOR CORNER REFLECTOR ANTENNA

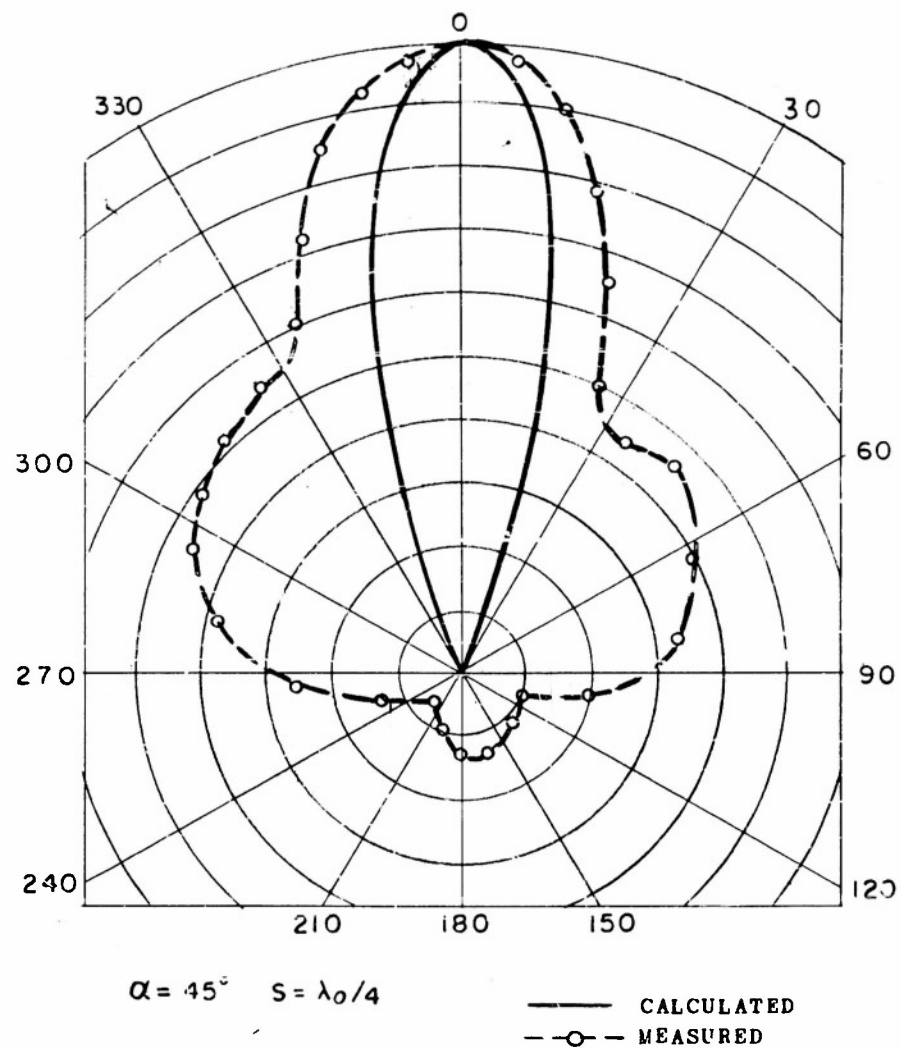


FIG. 16 MEASURED AND CALCULATED H-PLANE ELECTRIC FIELD
 FOR CORNER REFLECTOR ANTENNA

VIII TWO GAIN STANDARDS AND THEIR PERFORMANCES

8.1 Selection of the Gain Standards

The antennas obtained by setting the corner angle and the corner-to-dipole spacing of the variable corner reflector antenna to the sets of values (I), $\alpha = 90^\circ$, $s = \lambda_0/4$ and (II), $\alpha = 60^\circ$, $s = \lambda_0/2$ were calibrated as standard gain antennas for 800 to 1600 mc. Reasons for selecting the antennas defined by I and II are to be pointed out.

Because of their predicted optimum broad-band performances, (see page 19), the following antennas were considered for development as gain standards:

Antenna (a): $\alpha = 90^\circ$, $s = \lambda_0/4$

Antenna (b): $\alpha = 90^\circ$, $s = \lambda_0/2$

Antenna (c): $\alpha = 60^\circ$, $s = \lambda_0/2$

Antenna (d): $\alpha = 45^\circ$, $s = \lambda_0/2$

The results of the measurements described in the preceding chapter indicated that agreement between calculated and measured performances is poor for antenna (d) so that this antenna was eliminated. A good agreement between calculated and measured performances was indicated for antennas (a) and (b) and a fair agreement was indicated for antenna (c). (See Figs. 14a, 14b, and 15b).

Antenna (a) was selected over antenna (b) because a more favorable gain vs frequency characteristic was predicted for the former. (Compare curves of Fig. 7A.) Antenna (c) was selected primarily because it was felt that at least one antenna with corner angle different from 90° ought to be investigated further. But, in addition, expected similarity in the performances of antennas (a) and (b) was a reason for not selecting both of these antennas.

Description of further measurements of the performances of antennas (a) and (c) is presented on succeeding pages. For convenience, antenna (a) will be denoted as standard antenna I and antenna (c) as standard antenna II.

3.2 H-Plane Radiation Patterns of Standard Antenna I

and Standard Antenna II

H-plane radiation patterns of standard antennas I and II, measured at every 200 mc in the 800 mc-1600 mc band, are shown in Figs. 18a and, 18b, on page 36b, and in Figs. 20a and 20b, page 36d. In the measurement of these radiation patterns the standard antennas were used as receiving antennas at the transmission site pictured on Fig. 12. As already explained, this transmission site is very suitable for such measurements.

Calculated patterns for the highest and lowest frequencies in the band are included on Figs. 19a and 19e. It is seen that the calculated patterns for $f = 800$ mc almost coincide with those for $f = 1600$ mc. Moreover, it is a fact that these patterns enclose the patterns calculated for all frequencies in the band. Of course, such broad-band similarity in the above radiation patterns is to be expected of standard antennas I and II because of the constancy of their calculated gains as functions of frequency.

Comparison of the calculated and measured H-plane radiation patterns of the standard antennas will be deferred until the measurement of their E-plane radiation patterns and the calibration of their gains are described.

8.3 E-Plane Radiation Patterns of Standard Antenna I and Standard Antenna II

For measurement of E-plane radiation patterns, it was a practical expediency, if not almost a necessity, to revert to the testing method or technique illustrated on the next page. This was the case because of the difficulties that would be encountered in mounting standard antennas I and II for reception of horizontal polarization from directions parallel to the horizon. (The mounting fixture on the variable corner reflector antenna is located and is designed to provide ample support for mounting this antenna for vertical polarization, and consequently, for measurement of H-plane radiation patterns. See Figs. 10 and 11, also engineering drawing No. 5 of Fig. 24.) It is pertinent to mention that the elevated ground plane of Fig. 17 is a permanent installation of the Electronics Research Laboratory under whose auspices this research was conducted. No additional construction was required for the measurement of E-plane patterns of standard antennas I and II so that the matter of "practical expediency" mentioned above is now fully explained.

Equipment used in the measurements is as indicated in Fig. 17. Results were plotted by an automatic pattern recorder and are shown in Figs. 19a-19e for standard antenna I, and Figs. 21a through 21f, for standard antenna II.

The jagged variations seen in these patterns were no doubt caused by appreciable reflections from the ground plane and from the V-frame despite the fact that absorbing cloth was placed over these obstacles. The distance between the transmitting and receiving antennas was greater than $1.7 D^2/\lambda$ for the smallest wavelength used so that any variations in the patterns due to phase variation across the receiving apertures are probably masked by those due to the background reflections.

Calculated E-plane radiation patterns are shown on pages 36C and 36E. Comparisons of these calculated patterns with the measured E-plane patterns are not as significant as comparisons of calculated and measured H-plane patterns since the latter were measured in space almost entirely free of reflecting objects. However, the measured E-plane patterns give at least a first-approximation of the frequency dependence of the E-plane radiation.

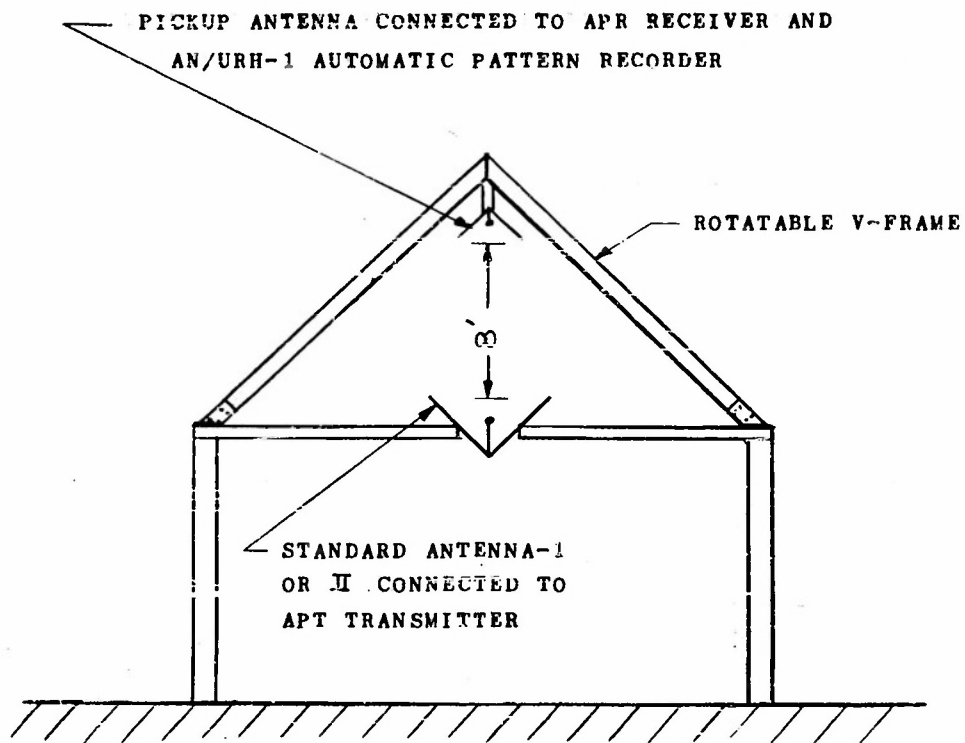
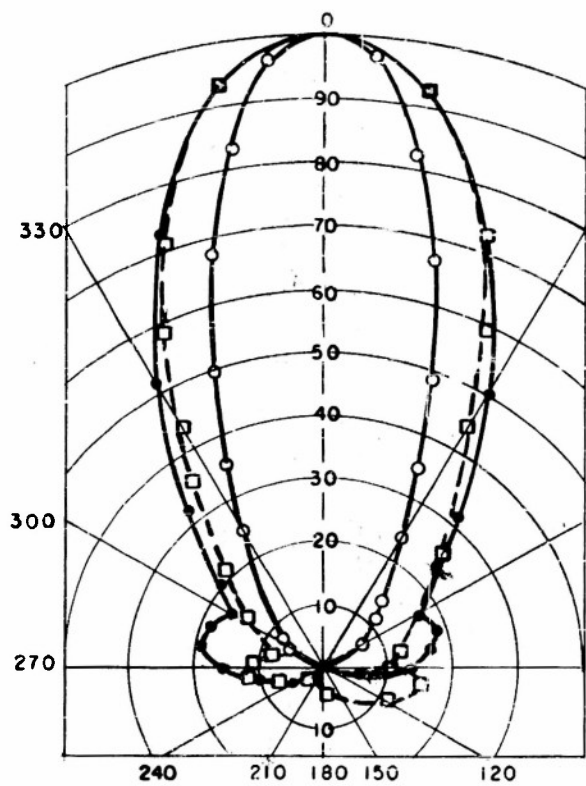
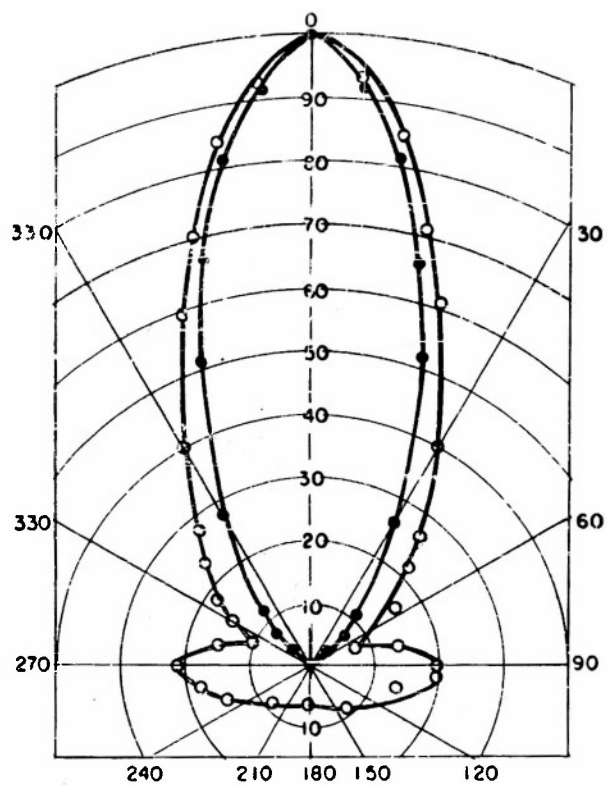


FIG. 17 TEST SET-UP FOR MEASUREMENT OF E-PLANE
RADIATION PATTERNS



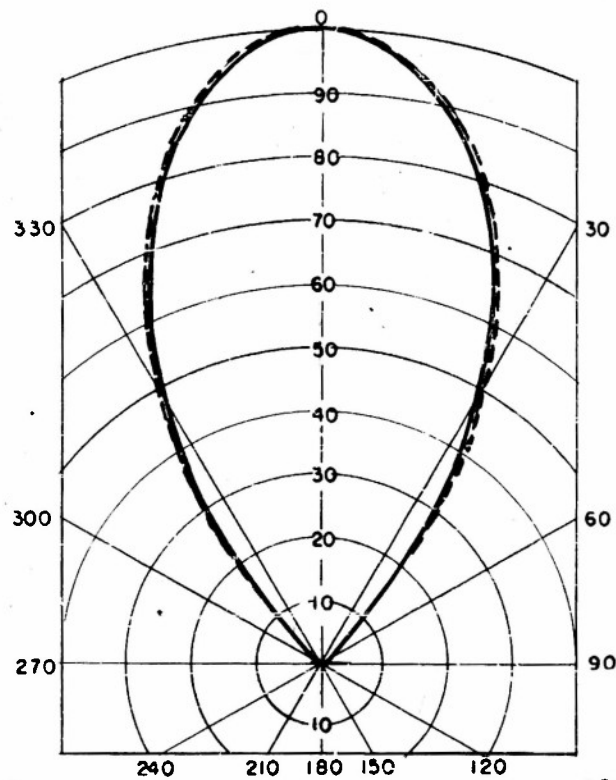
—●— 800 MC MEASURED
 - - - □ - - - 1000 MC
 —○— 1200 MC

18a



MEASURED —●— 1400 MC
 —○— 1600 MC

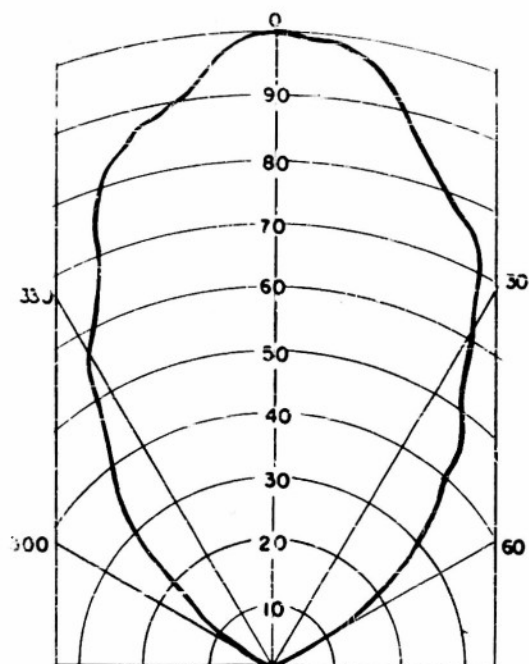
18b



CALCULATED - - - 800 MC
 — 1600 MC

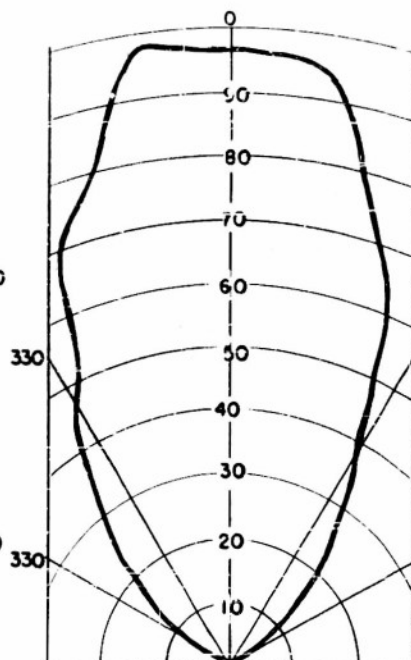
18c

FIG.18 MEASURED AND CALCULATED H-PLANE ELECTRIC FIELDS
FOR STANDARD ANTENNA - I



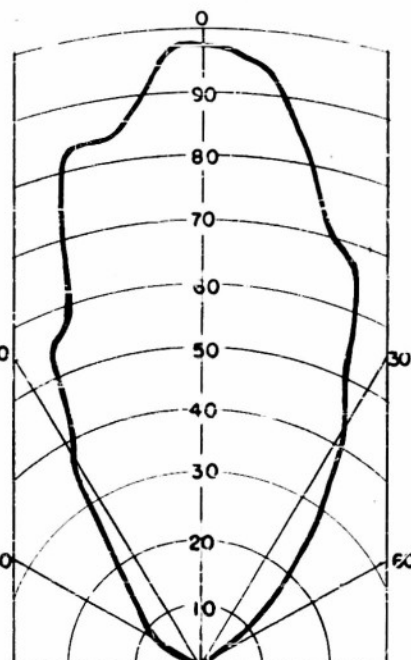
MEASURED (800 MC)

19a



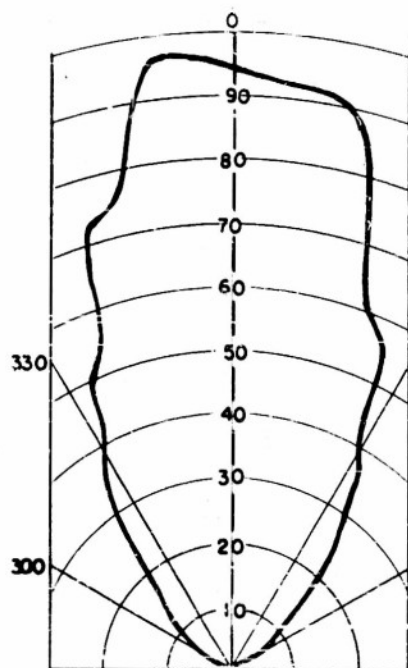
MEASURED (1000 MC)

19b



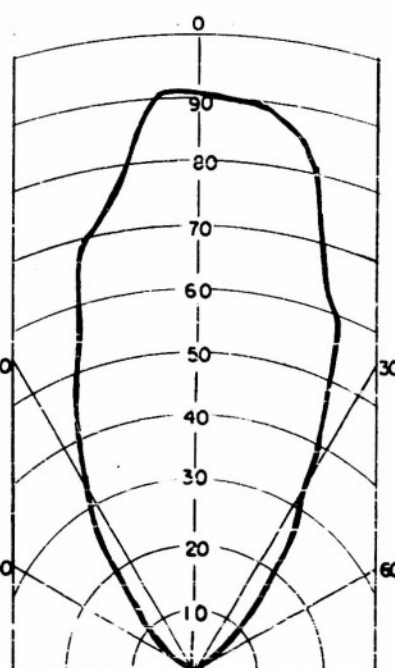
MEASURED (1200 MC)

19c



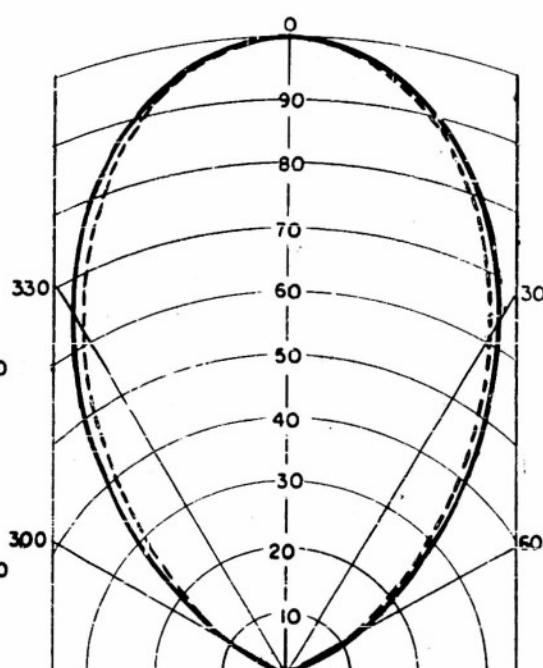
MEASURED (1400 MC)

19d



MEASURED (1600 MC)

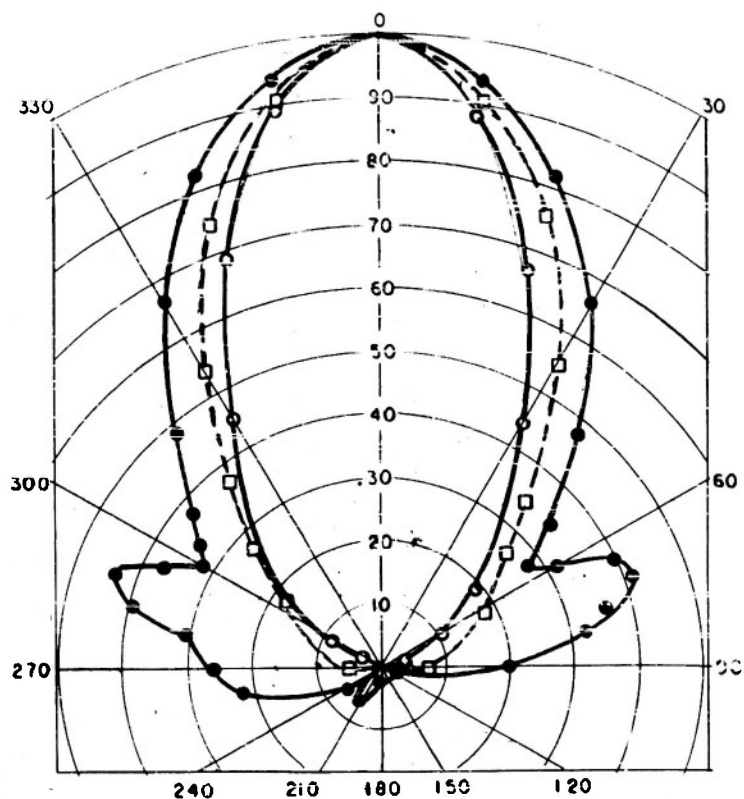
19e



CALCULATED — 800 MC
--- 1600 MC

19f

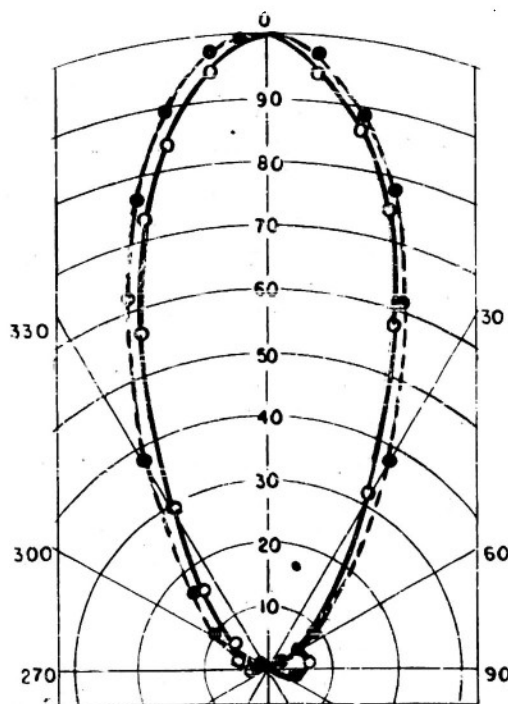
FIG. 19 MEASURED AND CALCULATED E-PLANE ELECTRIC FIELDS
FOR STANDARD ANTENNA - I



20a

MEASURED

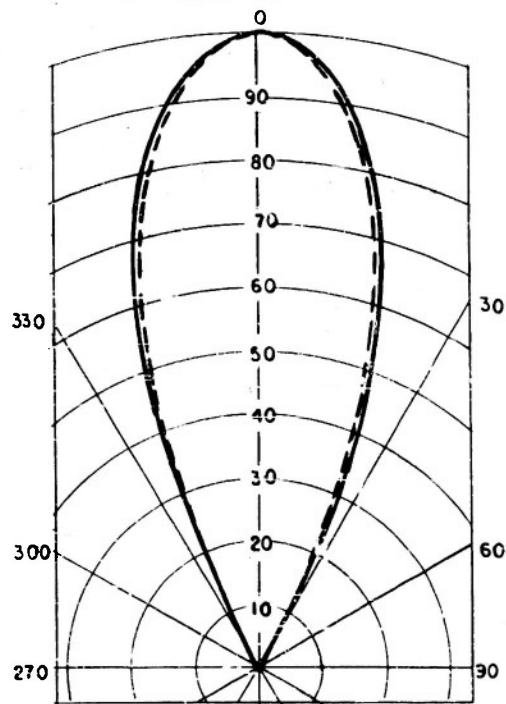
—●— 800 MC
 - - - □ - - 1000 MC
 —○— 1200 MC



20b

MEASURED

- - - ● - - 1400 MC
 —○— 1600 MC



20c

CALCULATED

- - - 800 MC
 — 1600 MC

FIG. 20 MEASURED AND CALCULATED H-PLANE ELECTRIC FIELDS
 FOR STANDARD ANTENNA-II

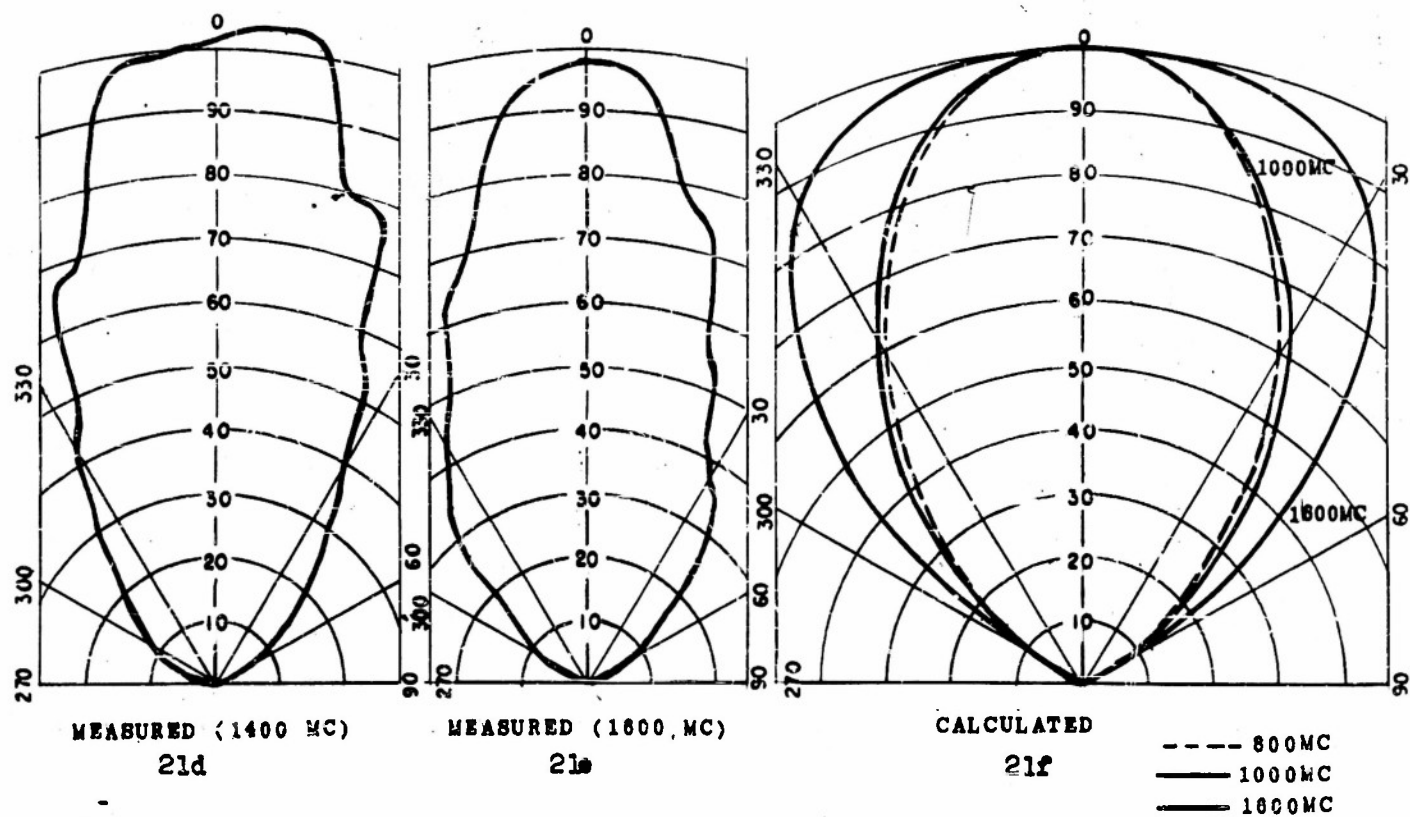
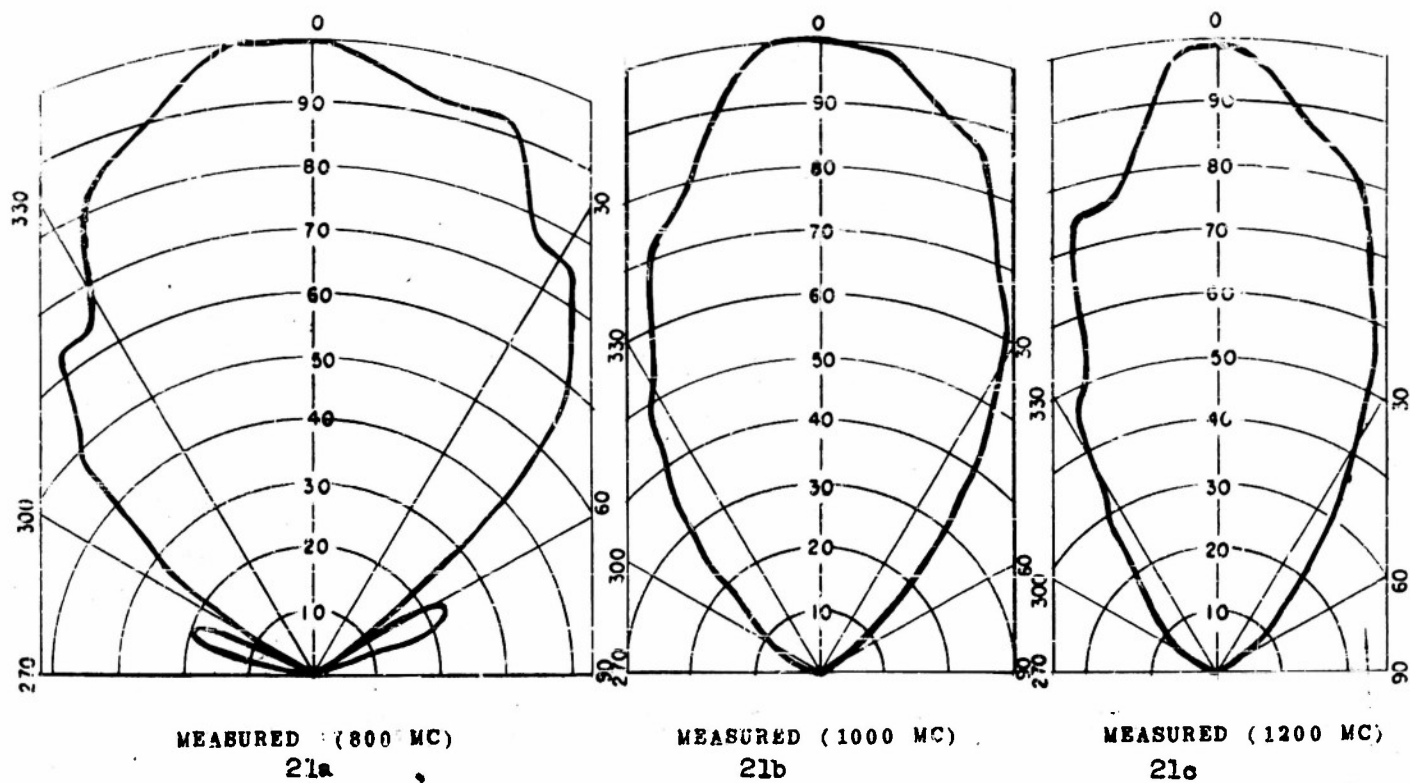


FIG. 21 MEASURED AND CALCULATED E-PLANE ELECTRIC FIELD FOR STANDARD ANTENNA-II

8.4 Gain Calibrations of Standard Antenna I and Standard Antenna II

Standard Antennas I and II were calibrated by the mirror method of gain determination. This method is based on the obvious fact that the echo or the intensity of the signal received by reflection from a large plane reflecting mirror is dependent upon the gain of the transmitting and receiving antenna. It is readily shown that the dependence is as given by the equation $G = 4\pi R |\Gamma| / \lambda$, where $R/2$ is the distance from the antenna aperture to the reflecting mirror, and Γ is the reflection coefficient set up in the antenna transmission line due to the reflected radiation. It is important to note that the test antenna and the signal generator should be matched to free space and to the transmission line, respectively, otherwise Γ will not be the consequence of only the radiation reflected from the mirror.

Gain measurements were conducted using the receiving equipment and the transmitter described in chapter VI. The transmitter was made to appear as a matched load to the reflected wave by employing a padder consisting of 75 feet of RG 58/U coaxial cable. This length of cable represented an attenuation of about 11 db at 800 mc and 15 db at 1600 mc. Additional equipment used included an impedance transformer for matching the standard antennas and a coaxial slotted line for measurement of $|\Gamma|$.

The reflecting mirror employed was a large relatively plane copper sheet of dimensions 7 1/3 ft. x 8 ft. This mirror was not perfectly planar; however, all deviations were very small compared to the wavelength so that little error was introduced on this account. The copper sheet and the equipment mentioned in the preceding paragraph are shown in Figs. 22a, 22b, and 22c, approximately at their respective test locations.

Gain measurements were made for frequencies of 600 mc, 900 mc, 1000 mc . . . 1600 mc at three nominal mirror to antenna distances, $R_1/2$, $R_2/2$, and $R_3/2$ so that an average value of gain could be obtained. Measurements were repeated at the three slightly greater distances $R_1/2 + \lambda/4$, $R_2/2 + \lambda/4$, and $R_3/2 + \lambda/4$ so that it would be possible to compensate for multiple reflection effects. The latter measurements are essential, as made clear in the following paragraph.



FIGURE 22a
TESTING SITE FOR
GAIN MEASUREMENTS

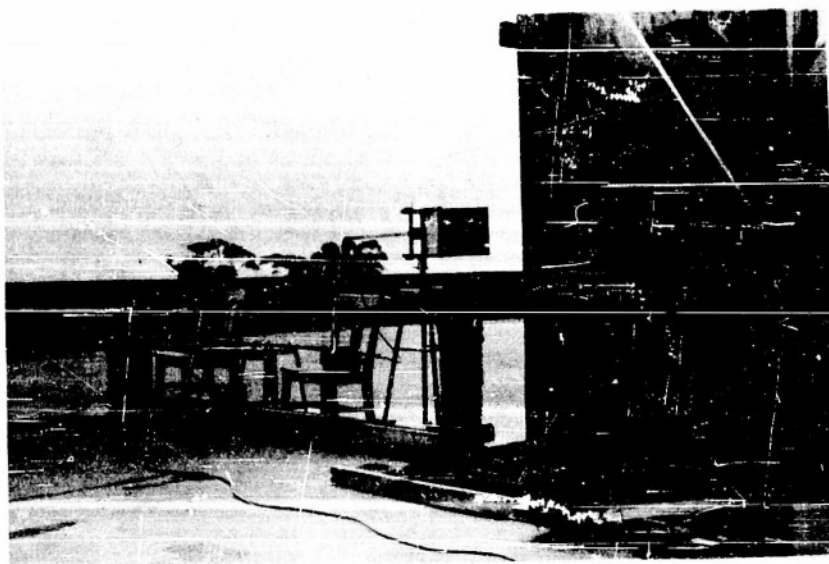


FIGURE 22b
GAIN MEASUREMENTS

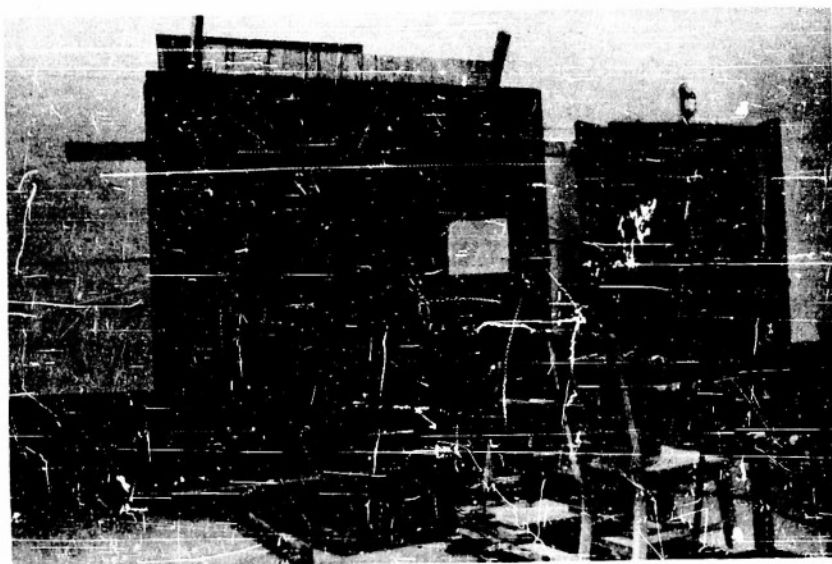


FIGURE 22c
STANDARD ANTENNA
AND ELECTRO-
MAGNETIC MIRROR

Radiation reflected from the mirror to the antenna is not all absorbed. The radiation not absorbed is scattered by the antenna so that a portion travels back to the mirror to be re-reflected toward the antenna, partially absorbed and re-scattered, and so on. The net effect of these multiple reflections is a cyclic variation of $|\Gamma|$ as a function of R with a period of $\lambda/2$.¹² Consequently, $G(R)$ and $G(R \pm \lambda/4)$ as calculated from the above equation are appreciably different unless R is so large that the amplitude of the first re-reflected wave is negligibly small compared to that of the primary reflected wave. It has been shown¹² that the true value of G is very nearly the geometric mean of $G(R)$ and $G(R + \lambda/4)$ or $G(R - \lambda/4)$ provided, of course, that R is sufficiently large ($R \gg 2D^2/\lambda$) so that phase variation across the antenna aperture is not excessive.

Other precautions were taken to improve the accuracies of the six reflection coefficients measured for each calibration frequency. These reflection coefficients were determined from voltage standing wave ratios measured near the center of the coaxial standing wave line so as to avoid edge effects at the ends of that slotted section. Each voltage standing wave ratio was calculated from the ratio of the geometric mean of two maximum values of response separated by a half wavelength to the minimum value between them. This procedure has been recommended^{2c} as it compensates for a standing wave distortion, known as "slope", which is usually present in coaxial slotted lines having even small eccentricities between their outer and inner conductors. To further improve the accuracy, a line stretcher and a shunt tuner were connected to the standing wave probe so as to permit standing wave detection with a tuned probe.

Brief mention of the determination of the transmission range and the wavelength remains to be made. The first of these quantities, taken as twice the distance from the mirror to the aperture planes of the standard antennas, was determined as precisely as possible using an ordinary tape measure. Wavelengths were calculated from the calibration frequencies which were set accurate to at least 2.5 mc. Actual tuning errors were probably smaller than 1.5 mc. In explanation, the APT transmitter was tuned to peak the output of the calibrated APR receiver whose 3 db bandwidth is approximately 3 mc; therefore, tuning errors were considerably smaller than 3 mc.

The gain calibration curves of standard antennas I and II are shown on Fig. 23, page 39A . Calibrated values of gain, indicated at every hundred megacycles on the curves, were arrived at by taking the arithmetic average of the geometric mean values of gain determined at the three nominal transmission ranges used. It is estimated that the calibrated gains are accurate to at least 0.25 db or six percent. Justification for this estimate of accuracy is given by the argument in the succeeding paragraph.

It is clear that gain measurements are performed at more than one transmission range for only one reason: an averaged gain can thereby be arrived at. Now, of course, it is implied that error in the measured data is reduced by the averaging process. It is believed that a reduction of error by a factor of (about) two is not overly optimistic for the gain measurements described in preceding paragraphs. Differences between the three geometric mean values of gain averaged to obtain a calibrated value were sometimes as large as ten percent so that overall calibration errors smaller than six percent are indicated.

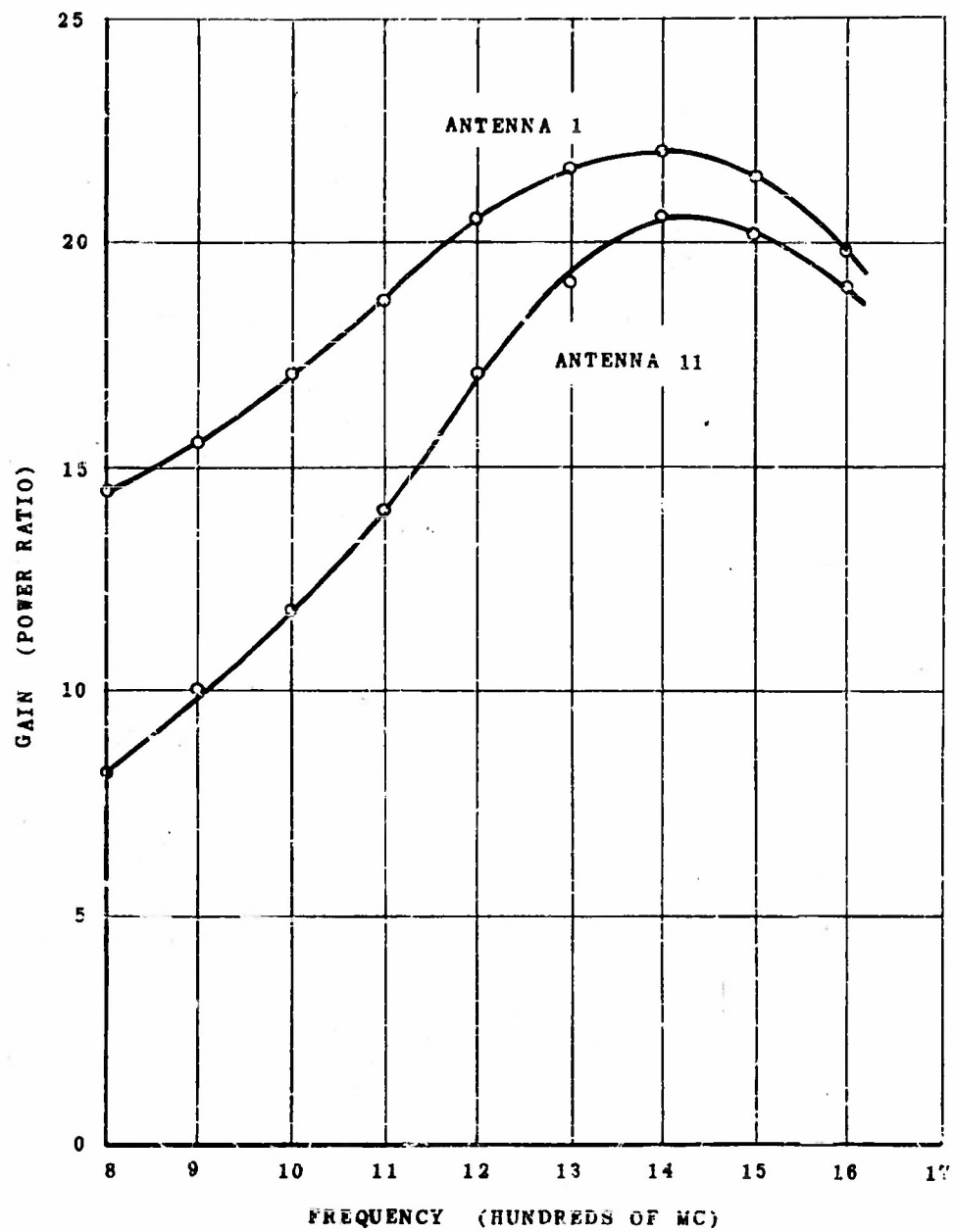


FIG. 23 STANDARD ANTENNA 1 & 11 - GAIN CALIBRATION

8.5 Comparison of Calculated and Measured Performance

The calculated performance of standard antenna I is a good approximation of its measured performance for the entire 800 mc - 1600 mc band. Comparison of the calculated and measured gain calibration curves, shown on Figs. 7a and 23a, reveals that maximum separations between the two gains occur approximately at 800 mc and 1400 mc, where the ratios of calculated gain to measured gain are only about 0.85 db and -0.85 db. Thus, the calculated gain differs from the measured gain by at most ± 22 percent.

It is significant to note that for frequencies near 1400 mc the gain was measured to be higher than calculated. The measured H-plane radiation patterns for frequencies of 1200 mc, 1400 mc, and 1600 mc (Figs. 18a and 18b) are compatible with the above result since the field intensity in the region $-30^\circ \leq \alpha \leq 30^\circ$ tapers off more rapidly than what is predicted by the calculated patterns (Fig. 18c). Of course, the total beam widths are larger than the 90° beam width of the calculated patterns; but apparently, the rapid decrease in field intensity at the small angles is more than sufficient to compensate for the small amount of radiation at the large angles, resulting in higher antenna gain than calculated.

The gain of standard antenna II is lower than that of the first standard antenna for all frequencies, as was expected. Of course, the reverse is true of the calculated gains so that the agreement between calculated and measured performance of standard antenna II is not as favorable as that of the other antenna. The difference between the gains of the two standard antennas is especially noticeable at frequencies below 1200 mc. At 800 mc, the gain of standard antenna I is almost twice that of standard antenna II. Also, it may be noted that for $f = 1000$ mc the ratio of the two gains is very nearly equal to the ratio of the receiving apertures, so that the illumination efficiencies are nearly equal at this frequency.

The maximum separation between calculated and measured gains of standard antenna II occurs at 800 mc where the calculated gain is higher by 5.3 db. However, for frequencies above 1300 mc these gains are equal to within one db.

Measured H-plane radiation patterns of standard antenna II correlate the observations of the previous two paragraphs. In the figures included in

Section 8.3, it is seen that for frequencies below 1200 mc the measured patterns are much broader than calculated, and also appreciably broader than corresponding patterns of standard antenna I. Secondly, for 1400 mc and 1600 mc measured and calculated patterns of standard antenna II are in close agreement.

8.6 Future Use of Standard Antennas I and II

During calibration, standard antennas I and II were mounted such that their feed antenna was five feet above the ground, a height chosen so that the antenna beams would be directed at a point near the center of the mirror. Obviously, when the standard antennas are used for gain comparisons they should be mounted at or near the height used during their calibration.

In a comparison measurement, the gain standards will have to be matched and this should be performed with the balun of the feed-antenna assembly set at 0.23λ . A final point in regard to the future use of the standard antennas is that both the dipole feed and the corner angle (of the variable corner reflector) can be adjusted accurately to the correct settings by employing either a 45° right triangle or a 30° right triangle. For example, in the case of standard antenna II, the corner reflector planes are wedged against the 60° angle of the 30° right triangle and the 30° angle of the latter is used to line up the feed-antenna on the bisector of the corner angle.

IX SUMMARY OF RESULTS

Theoretical analyses presented in this report were concerned with the determination of the performance of corner reflector antennas. The general solution for the far-zone field of a corner reflector antenna having any corner angle $\alpha = \frac{2\pi}{m}$, where m is any even integer, was derived assuming the reflecting planes of the corner reflector to be infinitely conductive and infinitely large. The Poynting vector of the electromagnetic field was determined from this far-zone field solution thereby permitting the well known Poynting vector method to be employed for the calculation of antenna gain.

Radiation resistance and antenna gain of dipole-fed 90° , 60° and 45° corner reflectors for several corner to dipole spacings were calculated for a two to one frequency band. Results of these comprehensive calculations predicted several combinations of corner angle and corner to dipole spacing that result in optimum, or at least very favorable, broad-band performances.

Following the analyses summarized above, it was shown that the solution of three definite integrals derived in Appendix A are useful in the general case. That is, the antenna gain and the radiation resistance of a corner reflector antenna of any corner angle α can be calculated using these definite integrals. In addition, it was shown that a considerable part of the data required in the calculations for the dipole-fed corner reflector is usable in corresponding calculations for a corner reflector illuminated by any feed antenna excited uniformly with azimuth.

Experimental investigations were conducted with two main objectives in mind, namely, to check calculated performances and to provide standard gain antennas for 800 to 1600 mc.

As a starting point, measurement of H-plane electric fields were made at a single frequency for each of the settings of corner angle and corner to dipole spacing (s) considered in the calculations. The immediate objective of these preliminary measurements was to obtain an idea as to which of the optimum combinations of α and s arrived at by calculation would result in better than acceptable actual performance.

Consideration of the results of the above measurements aided in the selection of the antennas that were calibrated as standard gain antennas,

and investigated thoroughly. The antennas defined by $\alpha = 90^\circ$, $s = 7.5$ cm and $\alpha = 60^\circ$, $s = 15$ cm, denoted as standard antenna I and standard antenna II, were the antennas selected. H-plane and E-plane radiation patterns of standard antennas I and II, and the gains of these antennas were measured throughout the 800 mc to 1600 mc band. Error in the gain calibration of both standard antennas was estimated to be within six percent for the entire band.

It was found that calculated performance is a good approximation of measured performance in the case of standard antenna I, and a good or bad approximation, depending on frequency, in the case of standard antenna II. The maximum separation between calculated and measured gain was only 0.85 db for the first standard antenna and as much as 5.3 db at 800 mc for the second. For frequencies above 1300 mc, however, calculated and measured gains of standard antenna II differed by less than one db. The large discrepancies between calculated and measured performances occurring at the lower frequencies in the case of the second standard antenna were attributed in part to its small receiving aperture compared to that of standard antenna I.

X CONCLUSIONS

The analysis presented in this report, added to that made by Kraus⁽⁴⁾, more or less determines the theoretical performance of corner reflectors illuminated by linear dipoles. Future analyses of corner reflectors might consider mainly other types of feed antennas.

In general, the higher antenna gains possible from corner reflector antennas when the corner angle is decreased from 90° will be attained in practice only if the reflector is made impractically large. For the relatively few cases where size is not of paramount importance, a 60° corner reflector may be practical provided that higher gain than obtainable from a 90° corner reflector antenna is required in the transmission system.

The good correlation between radiation patterns and antenna gains of the standard antennas calibrated during this research — that is, progressively broader patterns and progressively lower gains with decreasing frequency — discourages the possibility of greater calibration error than was estimated. For general purposes, standard antenna I should be preferred over standard antenna II. This conclusion follows from the fact that the first standard antenna exhibits the smaller variation in both antenna gain and radiation pattern with frequency. In addition, at the low calibration frequencies the gain of standard antenna I is substantially higher than that of the second standard antenna. Of course, the lower gain of standard antenna II may be in its favor when very low gain antennas such as dipoles are measured.

APPENDIX A

DERIVATIONS OF THE SOLUTIONS OF INTEGRALS REQUIRED TO CALCULATE THE PERFORMANCE OF CORNER REFLECTOR ANTENNAS

The integrals to be solved in this appendix are the following:

$$I_1 = \int_0^\pi \frac{[\cos(b \cos \theta) - \cos b]^2}{\sin \theta} d\theta = 2 \int_0^{\pi/2} [\cos(b \cos \theta) - \cos b]^2 d\theta$$

$$I_2 = \int_0^{2\pi} \cos[z \cos(\phi - c)] d\phi$$

$$I_3 = \int_0^{2\pi} \left\{ \sin[\rho \cos(\phi - b)] \right\} \left\{ \sin[\rho \cos(\phi - a)] \right\} d\phi$$

$$I_4 = \int_0^{2\pi} \left\{ \cos[\rho \cos(\phi - b)] \right\} \left\{ \cos[\rho \cos(\phi - a)] \right\} d\phi$$

where c , b , c , z , and ρ are constants.

I Solution of Integral I_1

Except for constant multipliers, integral I_1 may be recognized as the radiation resistance of a center-fed dipole. It is an interesting fact that the "self resistance" of the dipole, a popular term used in early investigations on linear antennas, is precisely the same as the radiation resistance obtained by integrating the normal component of the Poynting vector over the surface of a large sphere, provided that both resistances are referred to the same current. Indeed, Kraus^{10d} has recently shown that the method used to compute the self resistance is equivalent to an integration of the Poynting vector over the surface of the linear conductor (rather than over the surface of a large sphere). Thus, both methods should give the same answer since the power emanating from the large sphere is that radiated by the dipole source.

The method used in calculating the self resistance is termed the "induced emf method", and the integrals involved therein are quite different from I_1 .

Brown and King¹³ have obtained the expression for the dipole self resistance and it could be borrowed as the solution of Integral I_1 . However, since the integrals solved by Brown and King are different from I_1 and for the sake of continuity in discussions in the preceding thesis, it is felt that Integral I_1 should be evaluated.

Upon making the change of variable $u = \cos \theta$, I_1 becomes

$$I_1 = \int_1^{-1} \frac{(\cos b u - \cos b)^2 du}{(u+1)(u-1)}$$

$$I_1 = \int_1^{-1} \frac{(1+1/2 \cos 2b + 1/2 \cos 2bu - 2 \cos bu \cos b) du}{(u+1)(u-1)}$$

Or

$$I_1 = 1/2 \int_1^{-1} \frac{[(1+1/2 \cos 2b) + 1/2 \cos 2bu - 2 \cos bu \cos b] du}{u-1}$$

$$- 1/2 \int_1^{-1} \frac{[(1+1/2 \cos 2b) + 1/2 \cos 2bu - 2 \cos bu \cos b] du}{u+1}$$

Let $I_1 = I_{11} - I_{12}$, where I_{11} and I_{12} are the first and second of the above integrals. Making the changes of variable $u = x + 1$ in I_{11} and $u = -(x+1)$ in I_{12} yields

$$I_{11} = 1/2 \int_0^{-2} \left\{ (1 + 1/2 \cos 2b) + 1/2 \cos [2b(x+1)] - 2 \cos [b(x+1)] \cos b \right\} \frac{dx}{x}$$

$$I_{11} = -I_{12}$$

so that $I_1 = 2 I_{11}$. Substituting $y = -x$ gives

$$I_1 = \int_0^2 \left\{ (1+1/2 \cos 2b) + 1/2 \cos [2b(1-y)] - 2 \cos [b(1-y)] \cos b \right\} \frac{dy}{y}$$

$$I_1 = \int_0^2 (1+1/2 \cos 2b) \frac{dy}{y} + 1/2 \int_0^2 \cos[2b(1-y)] \frac{dy}{y} - 2 \int_0^2 \cos[b(1-y)] \frac{dy}{y}$$

$$I_1 = \int_0^2 (1+1/2 \cos 2b) \frac{dy}{y} + 1/2 \int_0^2 \cos 2b \cos 2by \frac{dy}{y} + 1/2 \int_0^2 \sin 2b \sin 2by \frac{dy}{y}$$

$$- 2 \int_0^2 \cos^2 b \cos by \frac{dy}{y} - 2 \int_0^2 \cos b \sin b \sin by \frac{dy}{y}$$

$$I_1 = I_{13} + I_{14} + I_{15} + I_{16} = I_{17}.$$

The integrals on the right hand side of this equation are solved separately below. In I_{14} through I_{17} , the change of variable $2by = z$ is made.

(a)

$$I_{13} = \int_0^2 (1+1/2 \cos 2b) \frac{dy}{y} = (1+1/2 \cos 2b) (\lim_{y \rightarrow 0} \ln y) \quad (1a)$$

(b)

$$I_{14} = \lim_{y \rightarrow 0} 1/2 \cos 2b \int_{2by}^{4b} \cos z \frac{dz}{z}$$

$$I_{14} = (1/2 \cos 2b) \left(\lim_{y \rightarrow 0} \int_{2by}^{\infty} \cos z \frac{dz}{z} - \int_{4b}^{\infty} \cos z \frac{dz}{z} \right)$$

$$I_{14} = -1/2 \cos 2b \left[\lim_{y \rightarrow 0} Ci(2by) - Ci(4b) \right],$$

where Ci denotes the cosine integral.

$$I_{14} = -1/2 \cos 2b \left[\gamma + \ln 2b + \lim_{y \rightarrow 0} \ln y - Ci(4b) \right], \quad (1b)$$

where γ = Euler's constant = .5772.

(c)

$$I_{15} = 1/2 \sin 2b \int_0^{4b} \sin z \frac{dz}{z} = \left[1/2 \sin 2b \right] \left[Si(4b) \right] \quad (1c),$$

where Si denotes the sine integral.

(d)

$$I_{16} = -2 \cos^2 b \lim_{y \rightarrow 0} \int_y^{2b} \cos \frac{z}{b} \frac{dz}{z}$$

$$I_{16} = -2 \cos^2 b \left(\lim_{y \rightarrow 0} \int_y^{\infty} \cos \frac{z}{b} \frac{dz}{z} - \int_{2b}^{\infty} \cos \frac{z}{b} \frac{dz}{z} \right)$$

$$I_{16} = 2 \cos^2 b \left[\lim_{y \rightarrow 0} Ci(b y) - Ci(2b) \right]$$

$$I_{16} = \left[1 + \cos 2b \right] \left[\gamma + \ln b + \lim_{y \rightarrow 0} \ln y - Ci(2b) \right] \quad (1d)$$

(e)

$$I_{17} = -2 \int_0^{2b} \cos b \sin b \sin \frac{z}{b} \frac{dz}{z} = -\sin 2b Si(2b) \quad (1e)$$

Collecting the solutions given by (1a) to (1e), and simplifying gives

$$I_1 = \left\{ \left[\gamma + \ln 2b - Ci(2b) \right] + \left[1/2 \sin 2b \right] \left[Si(4b) - Si(2b) \right] + 1/2 \cos 2b \left[\gamma + \ln b + Ci(4b) - 2 Ci(2b) \right] \right\} \quad (A.1)$$

If equation (A.1) is multiplied by sixty and b is replaced by $\frac{kl}{2}$, where $k = \frac{2\pi}{\lambda}$ and l = the length of the dipole, the result is the radiation resistance, R_{r_0} of the dipole referred to the current at an antinode. The self resistance determined by Brown and King must be multiplied by $2 \sin^2 kl/2$ to be equivalent to R_{r_0} . Multiplication by 2 is necessary because Brown and King considered grounded dipoles; and multiplication by $\sin^2 kl/2$ is necessary because the self resistance is referred to the current at the terminals of the dipole.

II Solution of Integral I_2

Integral I_2 is easily solved by making the change of variable $\phi - c = \beta$.

$$I_2 = \int_0^{2\pi} \cos \left[\frac{z}{\rho} \cos (\phi - c) \right] d\phi = \int_{-c}^{-c+2\pi} \cos (z \cos \beta) d\beta$$

The solution of the last integral is the well known result:

$$I_2 = 2\pi J_0(z) \quad (A.2)$$

where $J_0(z)$ is the zero order Bessel function of the first kind.

III Solution of Integral I_3

For convenience, the integral to be solved is restated below:

$$I_3 = \int_0^{2\pi} \left\{ \sin \left[\rho \cos (\phi - b) \right] \right\} \left\{ \sin \left[\rho \cos (\phi - a) \right] \right\} d\phi$$

The integrand of I_3 will be transformed through the use of the trigonometric identity

$$\sin x \sin y = 1/2 \left[\cos (x - y) - \cos (x + y) \right] \quad (3a)$$

By letting $\rho \cos (\phi - b) = x$ and $\rho \cos (\phi - a) = y$ there is obtained for the integrand of I_3

$$\begin{aligned} & \left\{ \sin [\rho \cos (\phi - b)] \right\} \left\{ \sin [\rho \cos (\phi - a)] \right\} \\ &= 1/2 \left[\cos \left\{ \rho [\cos (\phi - b) - \cos (\phi - a)] \right\} - \cos \left\{ \rho [\cos (\phi - b) + \cos (\phi - a)] \right\} \right] \end{aligned}$$

But

$$\begin{aligned} \cos (\phi - b) + \cos (\phi - a) &= (\cos b + \cos a) \cos \phi \\ &+ (\sin b + \sin a) \sin \phi, \quad \cos (\phi - b) - \cos (\phi - a) \\ &= (\cos b - \cos a) \cos \phi + (\sin b - \sin a) \sin \phi; \text{ and upon letting} \\ \rho(\cos b + \cos a) &= c, \quad \rho(\sin b + \sin a) = d, \quad \rho(\cos b - \cos a) = e, \text{ and} \\ \rho(\sin b - \sin a) &= f, \text{ the following result is obtained:} \end{aligned}$$

$$I_3 = 1/2 \int_0^{2\pi} [\cos(e \cos \phi + f \sin \phi) - \cos(e \cos \phi + d \sin \phi)] d\phi \quad (3b)$$

Now, it is seen that I_3 is the difference between two integrals of the form

$$I_{31} = \int_0^{2\pi} \cos [p \cos \phi + q \sin \phi] d\phi$$

Using $\cos \beta = \sum_{m=0}^{\infty} \frac{(-1)^m \beta^{2m}}{(2m)!}$ in I_{31} yields:

$$\begin{aligned} I_{31} &= \int_0^{2\pi} \left\{ \sum_{m=0}^{\infty} \frac{(-1)^m}{(2m)!} [p \cos \phi + q \sin \phi]^{2m} \right\} d\phi \\ &= \sum_{m=0}^{\infty} \frac{(-1)^m}{(2m)!} \int_0^{2\pi} [p \cos \phi + q \sin \phi]^{2m} d\phi \end{aligned}$$

The solution of the integral on the right hand side of the preceding equation is given by Bierens de Haan¹⁴ as follows:

$$\int_0^{2\pi} [p \cos \phi + q \sin \phi]^{2m} d\phi = \frac{\binom{2m}{2}}{2^{\binom{2m}{2}}} 2\pi [p^2 + q^2]^m$$

$$\text{where } 1^{\binom{2m}{2}} = (1) (3) (5) \dots (2m-1)$$

$$2^{\binom{2m}{2}} = (2) (4) (6) \dots (2m)$$

Therefore,

$$I_{31} = 2\pi \sum_{m=0}^{\infty} \frac{(-1)^m}{(2m)!} [p^2 + q^2]^m \frac{[(1) (3) (5) \dots (2m-1)]}{[(2) (4) (6) \dots (2m)]} \quad (3c)$$

Equation (3c) is simplified as follows:

$$I_{31} = 2\pi \sum_{m=0}^{\infty} (-1)^m \frac{[\sqrt{p^2 + q^2}]^{2m} [(1) (3) (5) \dots (2m-1)]}{[(1) (2) (3) (4) \dots (2m-1) (2) (4) (6) \dots (2m)]}$$

so that

$$\begin{aligned}
 I_{31} &= 2\pi \sum_{m=0}^{\infty} (-1)^m \frac{(\sqrt{p^2 + q^2})^{2m}}{[(2)(4)(6) \dots (2m)]^2} \\
 &= 2\pi \sum_{m=0}^{\infty} (-1)^m \frac{(\sqrt{p^2 + q^2})^{2m}}{[(2 \cdot 1)(2 \cdot 2)(2 \cdot 3) \dots (2 \cdot m)]^2} \\
 I_{31} &= 2\pi \sum_{m=0}^{\infty} (-1)^m \frac{(\sqrt{p^2 + q^2})^{2m}}{2^{2m} (m!)^2} = 2\pi J_0(\sqrt{p^2 + q^2})
 \end{aligned}$$

By applying this result to equation (3b), page 51, there is obtained

$$I_3 = \pi [J_0(\sqrt{e^2 + f^2}) - J_0(\sqrt{c^2 + d^2})]$$

$$\text{But } e^2 + f^2 = \rho^2 \left\{ [\cos a - \cos b]^2 + [\sin a - \sin b]^2 \right\}$$

Squaring the indicated terms and simplifying gives

$$\begin{aligned}
 e^2 + f^2 &= 2\rho^2 [1 - \cos(a-b)], \text{ so that} \\
 \sqrt{e^2 + f^2} &= \sqrt{2\rho^2 [1 - \cos(a-b)]} = 2\rho \sin\left(\frac{a-b}{2}\right)
 \end{aligned}$$

Similarly, it is easily shown that $\sqrt{c^2 + d^2} = 2\rho \cos\left(\frac{a-b}{2}\right)$.

The solution of I_3 , therefore, is given by equation (A.3) below:

$$I_3 = \pi \left\{ J_0 \left[2\rho \sin\left(\frac{a-b}{2}\right) \right] - J_0 \left[2\rho \cos\left(\frac{a-b}{2}\right) \right] \right\} \quad (A.3)$$

IV Solution of Integral I_4

Integral I_4 is restated below:

$$I_4 \int_0^{2\pi} \left\{ \cos \left[\rho \cos (\phi - b) \right] \right\} \left\{ \cos \left[\rho \cos (\phi - a) \right] \right\} d\phi$$

The solution of integral I_4 is immediately obtained by using the trigonometric identity

$$\cos x \cos y = 1/2 \left[\cos (x - y) + \cos (x + y) \right] \quad (4a)$$

On page 50, at the beginning of the analysis on integral I_3 , equation (3a) was used. Now, the second term on the right hand side of equation (3a) is preceded by a negative sign, whereas the corresponding term of equation (4a) is preceded by a positive sign. Except for this reversal of algebraic sign the right hand sides are identical. Therefore, the solution of integral I_4 is identical to that of integral I_3 except for a reversal of the algebraic sign preceding the second term; that is,

$$I_4 = \pi \left\{ J_0 \left[2\rho \sin \left(\frac{a-b}{2} \right) \right] + J_0 \left[2\rho \cos \left(\frac{a-b}{2} \right) \right] \right\} \quad (A.4)$$

APPENDIX B

SOLUTIONS FOR THE INTEGRALS DENOTED

BY I_m

On page 18 of this Report it is stated that the integrals there denoted by I_m could not be solved analytically. Now, of course, it was implied that systematic mathematical operations leading to a solution could be made. It might be worthwhile to point out that analytical solutions of I_m can be "arrived at" for all values of m .*

The integrals I_m were defined by the equation $R_r = R_{r0} + 120 I_m$, where R_r is the radiation resistance of a corner reflector antenna of corner angle $\alpha = \frac{2\pi}{m}$ and R_{r0} is the (free space) radiation resistance of the dipole feed antenna. Now, the circuit method used by Kraus and the Poynting vector method used by the writer must yield equivalent radiation resistances if resistance is referred to the same current. Therefore, the mathematical expressions obtained from the two methods can be equated to one another, so that I_m can be solved algebraically.

From the circuit method there is obtained⁴

$$R_r = \sum_{n=1}^{\infty} (-1)_n R_{1n} = R_{11} + \sum_{n=2}^{\infty} (-1)_n R_{1n} \quad (\text{B.1})$$

Where

R_{11} = Self resistance of the dipole feed antenna to be referred to the current at an antinode = R_{r0} ,
 R_{1n} = Mutual resistance between the dipole feed antenna and the n th image, the current at an antinode being used as the reference; and the notation $(-1)_n$ signifies that the algebraic sign of R_{1n} is chosen to agree with the phase of the excitation of the n th image.

Equating (b.1) to result ($R_r = R_{r0} + 120 I_m$) obtained by the Poynting vector method yields

$$I_m = \frac{1}{120} \sum_{n=2}^{\infty} (-1)_n R_{1n} \quad (\text{B.2}).$$

In equation (B.2)

*In the Report, emphasis is made that for practical purposes it is considerably more convenient to solve numerically the integrals I_m than to use the analytical solutions obtained in this appendix.

$$R_{1n} = 30 \left\{ (2)(2 + \cos k l) \text{Ci}(k d_n) - 4 \cos^2 \frac{k l}{2} \left[\text{Ci} \left[\frac{k}{2} (\sqrt{4 d_n^2 + l^2} - l) \right] + \text{Ci} \left[\frac{k}{2} (\sqrt{4 d_n^2 + l^2} + l) \right] \right] \right. \\
+ \cos k l \left[\text{Ci} \left[k (\sqrt{d_n^2 + l^2} - l) \right] + \text{Ci} \left[k (\sqrt{d_n^2 + l^2} + l) \right] + \sin k l \left[\text{Si} \left[k (\sqrt{d_n^2 + l^2} + l) \right] \right. \right. \\
\left. \left. - \text{Si} \left[k (\sqrt{d_n^2 + l^2} - l) \right] - 2 \text{Si} \left[\frac{k}{2} (\sqrt{4 d_n^2 + l^2} - l) \right] + 2 \text{Si} \left[\frac{k}{2} (\sqrt{4 d_n^2 + l^2} + l) \right] \right] \right\} \quad (\text{B.3})$$

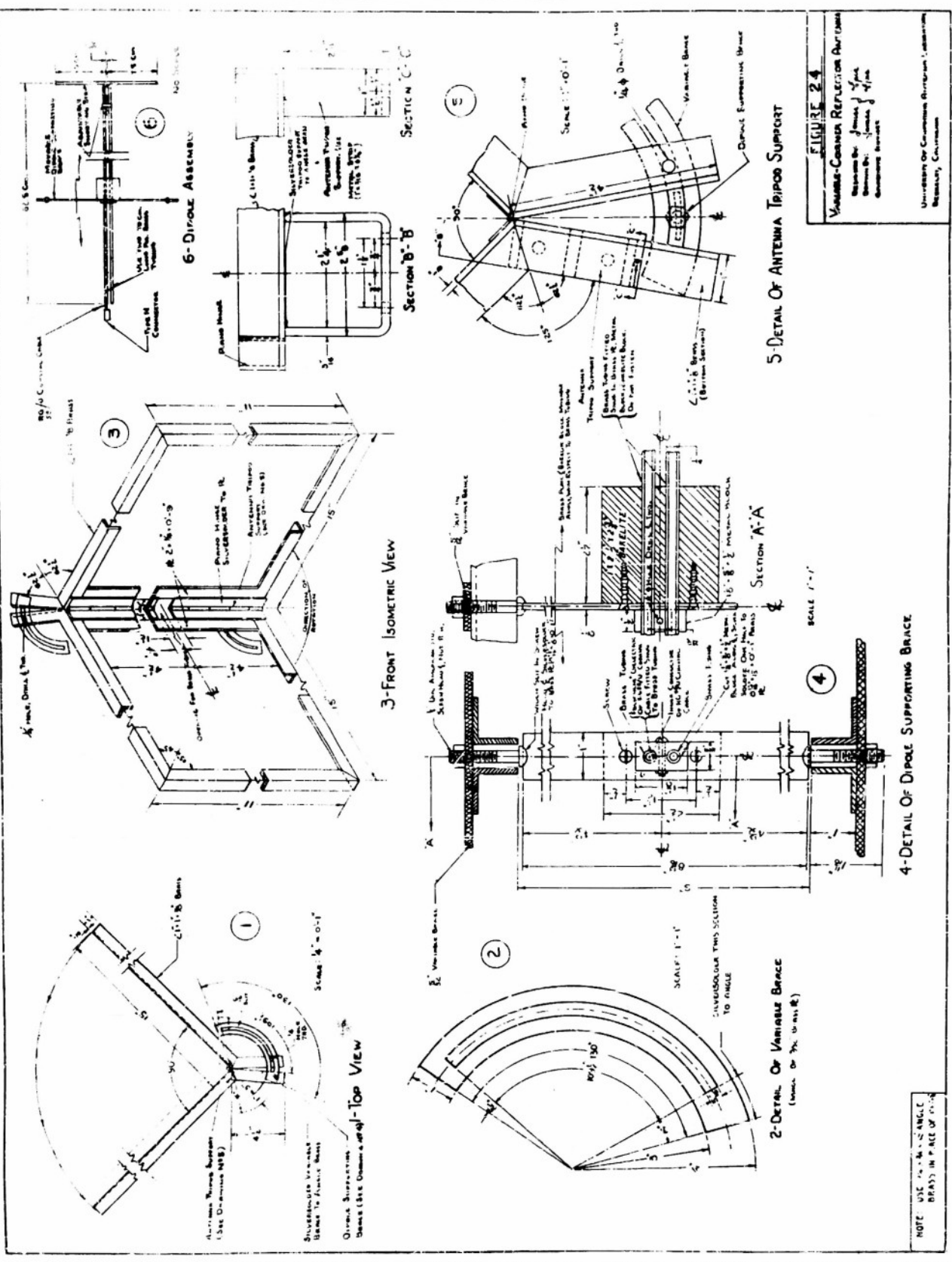
where d_n = spacing between the dipole and the n th image.

(Division of (B.3) by $2 \sin^2 \frac{k l}{2}$ gives the mutual resistance between two parallel, grounded dipoles referred to the terminal current; the mathematical derivation of this resistance is found in reference 13.)

For an example, the solution of I_m for $m = 4$ ($\alpha = 90^\circ$) will be obtained. From Fig. 3, page 12, it is clear that $d_2 = 2s$, and $d_3 = d_4 = 2s \sin 45^\circ = \sqrt{2}s$, so that $R_{13} = R_{14}$. Also, image 2 is positive and images 3 and 4 are negative. Therefore,

$$I_4 = \int_0^{\pi/2} \frac{[\cos(\frac{k l}{2} \cos \theta) - \cos \frac{k l}{2}]^2}{\sin \theta} \left[J_0(2 k s \sin \theta) - 2 J_0(\sqrt{2} k s \sin \theta) \right] d\theta \\
= \frac{1}{120} (R_{12} - 2R_{13}) - \frac{1}{4} \left\{ (2)(2 + \cos k l) \text{Ci}(2 k s) - 4 \cos^2 \frac{k l}{2} \left[\text{Ci} \left[\frac{k}{2} (\sqrt{16 s^2 + l^2} - l) \right] \right. \right. \\
\left. \left. \text{Ci} \left[\frac{k}{2} (\sqrt{16 s^2 + l^2} + l) \right] + \cos k l \left[\text{Ci} \left[k (\sqrt{4 s^2 + l^2} - l) \right] + \text{Ci} \left[k (\sqrt{4 s^2 + l^2} + l) \right] \right] \right. \right. \\
+ \sin k l \left[\text{Si} \left[k (\sqrt{4 s^2 + l^2} + l) \right] - \text{Si} \left[k (\sqrt{4 s^2 + l^2} - l) \right] - 2 \text{Si} \left[\frac{k}{2} (\sqrt{16 s^2 + l^2} + l) \right] \right. \\
\left. \left. + 2 \text{Si} \left[\frac{k}{2} (\sqrt{16 s^2 + l^2} - l) \right] \right] \right\} - \frac{1}{2} \left\{ (2)(2 + \cos k l) \text{Ci}(\sqrt{2} k s) - 4 \cos^2 \frac{k l}{2} \left[\text{Ci} \left[\frac{k}{2} (\sqrt{8 s^2 + l^2} - l) \right] \right. \right. \\
\left. \left. + \text{Ci} \left[\frac{k}{2} (\sqrt{8 s^2 + l^2} + l) \right] + \cos k l \left[\text{Ci} \left[k (\sqrt{2 s^2 + l^2} - l) \right] + \text{Ci} \left[k (\sqrt{2 s^2 + l^2} + l) \right] \right] \right. \right. \\
\left. \left. + \sin k l \left[\text{Si} \left[k (\sqrt{2 s^2 + l^2} + l) \right] - \text{Si} \left[k (\sqrt{2 s^2 + l^2} - l) \right] - 2 \text{Si} \left[\frac{k}{2} (\sqrt{8 s^2 + l^2} + l) \right] \right. \right. \right. \\
\left. \left. \left. + 2 \text{Si} \left[\frac{k}{2} (\sqrt{8 s^2 + l^2} - l) \right] \right] \right\} \right.$$

$$\begin{aligned}
& + \sin k l \left[\text{Si} \left[k(\sqrt{2s^2 + l^2} + l) \right] - \text{Si} \left[k(\sqrt{2s^2 + l^2} - l) \right] - 2\text{Si} \left[\frac{k}{2}(\sqrt{8s^2 + l^2} + l) \right] \right. \\
& \left. + 2\text{Si} \left[\frac{k}{2}(\sqrt{8s^2 + l^2} - l) \right] \right] \Bigg\} \qquad \qquad \qquad (\text{B.4})
\end{aligned}$$



BIBLIOGRAPHY

1. Cutler, C.C., King, A.P., and Kock, W.E., "Microwave Antenna Measurements," Proceedings of the I.R.E. XXXV (Dec. 1947), 1462-1471.
2. Silver, S., Microwave Antenna Theory and Design (1st ed., McGraw Hill, 1949), (a) page 580; (b) page 245; (c) page 549.
3. Montgomery, C.G., Technique of Microwave Measurements (1st ed., McGraw Hill, 1947), 907-914.
4. Kraus, J.D., "The Corner Reflector Antenna," Proceedings of the I.R.E., XXVIII (Nov. 1940), 513-519.
5. Interim Engineering Report, Sec. 4, (Ohio State University Antenna Laboratory, April 30, 1948), pages 4-9, 4-16.
6. Jeans, Sir James, Mathematical Theory of Electricity and Magnetism (5th ed., Cambridge University Press, 1925), 188.
7. Ramo, S., and Whinnery, J.R., Fields and Waves in Modern Radio, (J. Wiley and Sons, 1947), 122.
8. Tables of the Bessel Functions of the First Kind of Orders Zero and One (Harvard University Press, 1947).
9. Tables of Sine, Cosine, and Exponential Integrals, Vol. 1 and 2, 1940; Tables of Natural Logarithms, Vol. 3 and 4, 1941.
10. Kraus, J.D., Antennas, (1st ed., McGraw Hill, 1950), (a) page 333; (b) page 256; (c) page 334; (d) page 274.
11. Carter, P.S., "Circuit Relations in Radiating Systems and Applications to Antenna Problems," Proceedings of the I.R.E., XX (June 1932), 1004-1041.
12. Fippard, A.B., Burrell, O.J. and Cromie, E.E., "The Influence of Reradiation on Measurements of the Power Gain of an Aerial," Journal of I.E.E., XCIII, Part 3A, 720-723.
13. Brown, G.H. and King, R., "High Frequency Models in Antenna Investigations," Proceedings of the I.R.E., XX (April, 1934), 457-480.
14. Haan, Bierens de, Nouvelles Tables d'Integrales Definies, Integral No. 8, (G.E. Sterchert and Co., 1939), 104.

DISTRIBUTION LIST

Chief of Naval Research (Code 127)	2
Naval Research Laboratory (Code 2000)	6
Chief of Naval Research (Code 160)	1
Naval Research Laboratory (Code 5250)	1
O.N.R. Pasadena, California	1
O.N.R. San Francisco, California	1
O.N.R. Chicago, Illinois	1
O.N.R. New York, New York	1
O.N.R. Fleet Post Office, New York	2
Chief, Bureau of Ordnance (Re4)	1
Chief, Bureau of Ships (Code 838)	2
Chief, Bureau of Aeronautics (EL-51)	1
Chief of Naval Operations (Op-371)	1
Chief of Naval Operations (Op-30)	1
Chief of Naval Operations (Op-92)	1
Naval Ordnance Laboratory, White Oak, Maryland	1
U.S.N.E.L. San Diego, California	1
Naval Air Development Center, Johnsville, Pennsylvania (AAEL)	1
U.S. Naval Post Graduate School, Monterey, California (Librarian)	1
U.S. Coast Guard (EEE)	1
Research and Development Board	1
Armed Services Technical Information Agency	5
Office of Technical Services	1
National Bureau of Standards, Dr. N. Smith	1
Dept. of EE, Cornell University, Dr. H.G. Booker	1
Dept. of EE, University of Illinois, Prof. E.C. Jordan	1
Mass. Institute of Technology, Mr. J. Hewitt	1
Stanford Research Institute, Dr. J.V.N. Granger	1
Dept. of EE, University of Texas	1
Watson Laboratories Library, AMC, (ENAGSI)	1
Institute of Mathematical Sciences, N.Y.U., Mr. N. Chako	1
E.R.L. Stanford University, Dr. F.E. Terman	1
Mathematics Research Group, N.Y.U., Dr. M. Kline	1
Office of the Chief Signal Officer, Pentagon, (SIGET)	1
Signal Corps Engineering Laboratories, Mr. G.C. Woodyard	1
Air Force Cambridge Research Center (CRRF)	1
Air Research and Development Command (RDTRR)	1
Air Research and Development Command (HDTDRR)	1
Air Research and Development Command (RDTDRR)	1
Wright Air Development Center (WCLC)	1
Wright Air Development Center (WCLRC)	1
Craft Laboratory, Harvard University, Prof. R.W.P. King	1
Antenna Laboratory, Ohio State University, Dr. Tai	1
Brooklyn Polytechnic Institute, Dr. A. Oliner	1
White Sands Annex, Ballistic Research Laboratory, Mr. M.A. Krivanich	1
Squier Signal Laboratory, Mr. V.J. Kublin	1
Rome Air Development Center, Griffis Air Force Base (RCRW)	1
Ballistic Research Laboratory, Aberdeen Proving Ground	1
Bell Telephone Laboratories, Murray Hill, Mr. J.R. Wilson	1
Institute of Mathematical Sciences, N.Y.U. Mr. N. Chako	1

Armed Services Technical Information Agency

Because of our limited supply, you are requested to return this copy WHEN IT HAS SERVED YOUR PURPOSE so that it may be made available to other requesters. Your cooperation will be appreciated.

AD

45449

NOTICE: WHEN GOVERNMENT OR OTHER DRAWINGS, SPECIFICATIONS OR OTHER DATA ARE USED FOR ANY PURPOSE OTHER THAN IN CONNECTION WITH A DEFINITELY RELATED GOVERNMENT PROCUREMENT OPERATION, THE U. S. GOVERNMENT THEREBY INCURS NO RESPONSIBILITY, NOR ANY OBLIGATION WHATSOEVER; AND THE FACT THAT THE GOVERNMENT MAY HAVE FORMULATED, FURNISHED, OR IN ANY WAY SUPPLIED THE SAID DRAWINGS, SPECIFICATIONS, OR OTHER DATA IS NOT TO BE REGARDED BY IMPLICATION OR OTHERWISE AS IN ANY MANNER LICENSING THE HOLDER OR ANY OTHER PERSON OR CORPORATION, OR CONVEYING ANY RIGHTS OR PERMISSION TO MANUFACTURE, USE OR SELL ANY PATENTED INVENTION THAT MAY IN ANY WAY BE RELATED THERETO.

Reproduced by
DOCUMENT SERVICE CENTER

UNCLASSIFIED